

Simulation of Viscous Fingering during WAG in Presence of Asphaltene

by

Muhammad Farid bin Ahmad Tarmizi

**Dissertation submitted in partial fulfillment of
the requirements for the
Bachelor of Engineering (Hons)
(Petroleum Engineering)**

MAY 2011

**Universiti Teknologi PETRONAS
Bandar Seri Iskandar
31750 Tronoh
Perak Darul Ridzuan**

CERTIFICATION OF APPROVAL

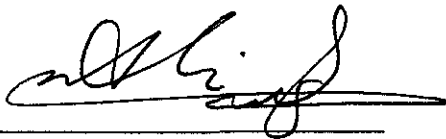
Simulation of Viscous Fingering during WAG in Presence of Asphaltene

by

Muhammad Farid bin Ahmad Tarmizi

A project dissertation submitted to the
Petroleum Engineering Programme
Universiti Teknologi PETRONAS
in partial fulfillment of the requirement for the
BACHELOR OF ENGINEERING (Hons)
(PETROLEUM ENGINEERING)

Approved by,

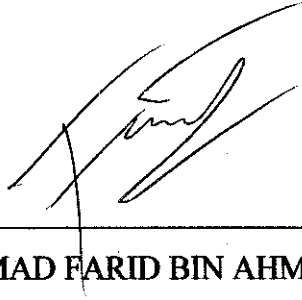


(MR. ALI F. MANGI ALTA'EE)

UNIVERSITI TEKNOLOGI PETRONAS
TRONOH, PERAK
May 2011

CERTIFICATION OF ORIGINALITY

This is to certify that I am responsible for the work submitted in this project, that the original work is my own except as specified in the references and acknowledgements, and that the original work contained herein have not been undertaken or done by unspecified sources or persons.

A handwritten signature in black ink, appearing to read 'Muhammad Farid Bin Ahmad Tarmizi', is written over a horizontal line.

MUHAMMAD FARID BIN AHMAD TARMIZI

ABSTRACT

Asphaltene precipitation and viscous fingering are two serious problems encountered during gas injection. The objective of this project is to study the effect of asphaltene deposition on viscous fingering and oil recovery. This project includes critical literature review and simulation work. The simulation work has been done using a compositional oil simulator, CMG GEM. Two types of formation have been modeled; without asphaltene deposition and with asphaltene deposition. Fluid flow through the two formations has been simulated to observe viscous fingering that happens during carbon dioxide (CO₂) injection and water-alternating-gas (WAG) injection. Results show that presence of asphaltene slows down the propagation of viscous fingering and production of oil. At a similar injected pore volume (PVI), presence of asphaltene does not change the shape and size of viscous fingering during CO₂ injection but it slightly changes the shape and size of viscous fingering during different types of WAG injection. In addition, less fingering is observed at higher WAG ratio and severe fingering is observed in the case of CO₂ injection and lower WAG ratio.

ACKNOWLEDGEMENTS

The author would like to give a big thank to his supervisor, Mr. Ali F. Mangi Alta'ee, lecturer from Department of Geoscience and Petroleum Engineering, Universiti Teknologi PETRONAS for his kind supervision and assistance in completing this project and for suggesting the research topic. The author would like to thank him also for introducing and suggesting the use of simulation software by Computer Modelling Group Ltd. (CMG) for this project. Special thank to Reservoir Simulation Engineers from CMG Software Support; Amir Moradi, Kourosh Shahhoseiny, Abe Doroudi and Dwarak Uthayashankar for all their help in using the software.

TABLE OF CONTENTS

| | |
|--|------------|
| CERTIFICATION OF APPROVAL..... | i |
| CERTIFICATION OF ORIGINALITY..... | ii |
| ABSTRACT..... | iii |
| ACKNOWLEDGEMENTS..... | iv |
| | |
| 1. CHAPTER 1 – INTRODUCTION | |
| 1.1 Background of Study..... | 1 |
| 1.2 Problem Statement..... | 3 |
| 1.3 Objectives and Scope of Study..... | 4 |
| 1.4 Relevancy and Feasibility of Study..... | 5 |
| | |
| 2. CHAPTER 2 – LITERATURE REVIEW AND THEORY | |
| 2.1 Viscous Fingering..... | 6 |
| 2.1.1 Simulation of Viscous Fingering..... | 7 |
| 2.2 Gas Injection (EOR)..... | 9 |
| 2.3 Asphaltene..... | 13 |
| 2.3.1 Definition..... | 13 |
| 2.3.2 Where asphaltene desposits are found?..... | 13 |
| 2.3.3 Relation between Asphaltene and Resin..... | 14 |
| 2.3.4 Relation between CO ₂ Concentration and Asphaltene Precipitation..... | 15 |
| 2.3.5 Asphaltene Precipitation, Flocculation and Deposition..... | 16 |
| | |
| 3. CHAPTER 3 – METHODOLOGY | |
| 3.1 Research Methodology..... | 17 |
| 3.1.1 Brief Explanation on Simulation Work..... | 18 |
| 3.2 Tools Required..... | 20 |
| 3.3 Project's Gantt Chart and Key Milestones..... | 21 |

LIST OF FIGURES

| | |
|--|----|
| Figure 1: Viscous fingering in a Hele-Shaw cell..... | 1 |
| Figure 2: Illustration of WAG process..... | 10 |
| Figure 3: Research flowchart..... | 17 |
| Figure 4: Main simulations for this project..... | 19 |
| Figure 5: Example of oil compositions and properties..... | 20 |
| Figure 6: Gantt chart with key milestones..... | 21 |
| Figure 7: Modeled asphaltene precipitation as a function of pressure for Oil 1..... | 31 |
| Figure 8: Modeled asphaltene precipitation as a function of pressure for Oil 2..... | 31 |
| Figure 9: 80 x 1 x 20 grid block configuration (Length/height = 16)..... | 34 |
| Figure 10: Colour scale used in showing CO ₂ distribution across formation..... | 36 |
| Figure 11: Colour scale used in showing oil saturation across formation..... | 36 |
| Figure 12: Oil saturation at 0.10 PVI (left) and 0.20 PVI (right)..... | 38 |
| Figure 13: Oil saturation after 30 days of CO ₂ injection..... | 38 |
| Figure 14: Cumulative oil produced, bbl vs. time..... | 39 |
| Figure 15: Injector gas rate, ft ³ /day vs. time..... | 39 |
| Figure 16: Producer oil rate, bbl/day vs. time..... | 40 |
| Figure 17: Oil saturation at 0.10 PVI (left) and 0.15 PVI (right)..... | 41 |
| Figure 18: Oil saturation after 30 days of 1:1 WAG injection..... | 42 |
| Figure 19: Cumulative oil produced, bbl vs. time..... | 42 |
| Figure 20: Injector gas rate, ft ³ /day vs. time..... | 43 |
| Figure 21: Injector water rate, bbl/day vs. time..... | 43 |
| Figure 22: Producer oil rate, bbl/day vs. time..... | 44 |
| Figure 23: Oil saturation at 0.10 PVI (left) and 0.15 PVI (right)..... | 45 |
| Figure 24: Oil saturation after 30 days of 1:2 WAG injection..... | 46 |
| Figure 25: Cumulative oil produced, bbl vs. time..... | 46 |
| Figure 26: Injector gas rate, ft ³ /day vs. time..... | 47 |
| Figure 27: Injector water rate, bbl/day vs. time..... | 47 |
| Figure 28: Producer oil rate, bbl/day vs. time..... | 48 |
| Figure 29: Oil saturation at 0.10 PVI (left) and 0.15 PVI (right)..... | 49 |

CHAPTER 1

INTRODUCTION

1.1 Background of Study

Viscous fingering is the unstable displacement of a more viscous fluid by a less viscous fluid. The fingering of an injection fluid into an in-situ fluid can influence reservoir flow behavior and adversely impact recovery. If a low viscosity fluid is injected into a cell containing a high viscosity fluid, the low viscosity fluid will begin to form fingers as it moves through the fluid. It will not uniformly displace the higher viscosity fluid. These fingers can have different shapes. ^[1]

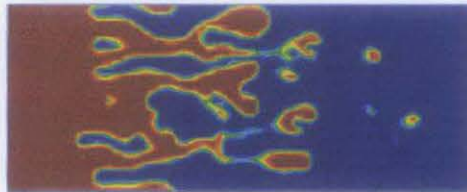


Figure 1: Viscous fingering in a Hele-Shaw cell

Source: <http://www.ulb.ac.be/cenoliw3/spatio.html>

Asphaltene is the heavy component of a crude oil that constitutes a potential problem because of its tendency to precipitate and deposit causing formation damage and blockage in tubular, pipelines and surface facilities leading to decline in oil production. Asphaltene is insoluble in n-pentane or n-hexane, but is soluble in toluene or benzene. Asphaltene precipitation and deposition can cause serious problems.

Abdallah *et al.* (2010) ^[2] reported in their paper that there are numbers of wells affected with asphaltene in an onshore field in Abu Dhabi and this is likely to increase in the future implementation of artificial lift and gas injection for enhanced oil recovery (EOR). Another paper by Oskui, Jumaa & Abuhaimed (2009) ^[3] reported that Kuwait Oil Company (KOC) is facing asphaltene deposition problems in the wellbore of some

of the Marrat Jurassic reservoirs in West Kuwait, South East Kuwait and North Kuwait. This has caused a reduction in production and shutting of some of the wells and a severe detrimental effect on the economics of oil recovery. ^[3]

EOR is the method for increasing the amount of crude oil that can be extracted from an oil field. Using EOR, 30-60% or more of the original oil in place can be extracted compared with only 20-40% if using primary and secondary recovery. Its function is not only to restore formation pressure, but also to improve oil displacement or fluid flow in the reservoir. ^[4] The three major types of enhanced oil recovery operations are chemical flooding, miscible displacement (carbon dioxide injection or hydrocarbon injection) and thermal recovery. ^[4] Water alternating gas process (WAG) is one type of EOR.

Simulation work has been done using a simulation software by Computer Modelling Group Ltd (CMG) to simulate viscous fingering during CO₂ and WAG injection in presence of asphaltene deposition.

1.2 Problem Statement

Viscous fingering is an undesirable phenomenon during gas injection. It leads to poor sweep efficiency, early water breakthrough and slow oil recovery rate. ^[5] The mobility/viscosity difference between the injected and displaced fluids is the cause of the fingering.

Asphaltene precipitation is another undesirable thing that happens during the injection of gas into the reservoir to displace oil. Asphaltene precipitation and deposition alters formation porosity, wettability and induces near-wellbore formation damage where permeability of the formation is reduced. As recognized by Boer *et al.* (1992) ^[6], light oil with small amount of asphaltene is more likely to cause problems during production than heavy oil even though heavy oil has larger amount of asphaltene.

Viscous fingering and asphaltene precipitation are two serious problems that happen during gas injection. In this project, the relation between asphaltene deposition and viscous fingering is studied. The study is to know whether presence of asphaltene deposition in the reservoir affects the size and shape of viscous fingering. Since no literature on the relationship between asphaltene deposition and viscous fingering was found, this study can be considered one of a kind.

1.3 Objectives and Scope of Study

The objectives of this study are:

- a. To simulate viscous fingering using a compositional oil simulator for a formation with presence of asphaltene deposition
- b. To study on the effect of asphaltene deposition on viscous fingering during CO₂ injection and WAG injection
- c. To study the effect of asphaltene deposition on oil recovery

The scope of study includes the following:

- a. Literature review on asphaltene, viscous fingering and enhanced oil recovery
- b. Familiarization of compositional oil simulator software
- c. Modeling of asphaltenic light oil using fluid modeling software, WinProp
- d. Conducting simulations of viscous fingering during CO₂ and WAG injections
- e. Comparison of viscous fingering and oil recovery between two types of formation; formation without asphaltene deposition and formation with asphaltene deposition for each type of injection method

1.4 Relevancy and Feasibility of Study

This study is on the effect of asphaltene precipitation and deposition on viscous fingering during WAG. Viscous fingering is an unavoidable problem encountered during gas injection that can reduce the speed of oil recovery. Asphaltene precipitation happens when gas is injected into oil reservoir hence induced oil instability. It causes problems from oil production to oil processing. It is known that gas injection is one of the most common EOR process used to improve oil recovery. The two problems pose serious threats to the efficiency of oil recovery till now.

In this study, the effect of asphaltene deposition on viscous fingering and oil recovery is studied. If asphaltene deposition is proved to have negative effects on viscous fingering and oil production, steps may be taken to reduce or prevent asphaltene deposition for future EOR program.

This study is expected to be feasible because of the followings:

- a. Papers and journals for referencing purpose can be downloaded from the website, www.onepetro.org without any charge imposed to the student.
- b. The simulation software (by CMG) required for the simulation work is available in computer laboratory at Academic Block 15 complete with how-to-use manual.
- c. Since the study is on the simulation of viscous fingering, no other materials other than the software and a computer are needed.

CHAPTER 2

LITERATURE REVIEW AND THEORY

2.1 Viscous Fingering

Fingering often occurs in an injection project. It is an occurrence where the injected fluid does not contact with the entire reservoir but bypasses sections of the reservoir fluids in finger-like manner. Because of portions of the reservoir are not contacted by the injection fluid (poor sweep efficiency), fingering is not desirable. If viscous fingering happens, considerable quantities of gas are needed to displace all the oil which makes the process expensive and time consuming.

Viscous fingering happens when a less viscous fluid, such as gas or water, is injected to displace a more viscous one, such as oil. However in the inverse scenario, no fingering patterns are form due to stable interface between the fluids in contact. In a reservoir, viscous fingering may be triggered by variations in permeability. ^[5]

The selection of the displacing fluid with particular characteristics becomes extremely significant in avoiding the growth and the propagation of finger-patterned flow, which leads to extremely poor displacement efficiency in both miscible and immiscible displacement for EOR. Fingering can be a reservoir heterogeneity problem or a fluid displacement problem. ^[1] The physical instability causing viscous fingering is driven by the adverse mobility ratio across a fluid front.

Alternating injection of water and gas reduces the effect of viscous fingering by reducing the mobility contrast between the fluids. Experiments by Naami, Catania & Islam (1999) ^[8] detected the existence of heterogeneity fingers. From their experimental study, it was found that viscous fingers travel much faster than heterogeneity fingers.

2.1.1 Simulation of Viscous Fingering

Tchelepi and Orr Jr. (1993) in their study ^[10] did two- and three-dimensional computations with a hybrid finite-difference/particle tracking technique. The two- and three-dimensional simulations were compared for unstable displacements. In both homogeneous and heterogeneous porous media, gravity segregation is much more effective in 3D than in 2D computations.

Moissis *et al.* (1998) ^[11] studied the viscous finger in miscible displacement. In their study, they used numerical simulation for studying viscous fingering. They found that the local permeability distribution near the entrance of the porous medium plays an important role in finger generation and the number of developing fingering and their growth rates depend strongly on the mobility ratio.

The miscible displacement in porous media has been simulated by Ku *et al.* (1989) ^[12] using pseudospectral matrix element method for displacing fluid in a horizontal slab and five-spot reservoirs. Compared to the case of uniform permeability, the region with higher permeability will induce the less viscous fluid with a faster speed, and hence a fingered front is appeared earlier as expected in the case of heterogeneous permeability. From the study, it was found that the less viscous finger with a higher permeability will shield the viscous one with a lower permeability and then both will merge into a single finger. For quartet five-spot reservoir, even without the perturbation of permeability, a finger still exists due to different fluid path caused by the geometrical effect.

Blunt *et al.* (1992) ^[23] have developed a predictive theory that reduces to the Todd and Longstaff (1971) ^[24] model to account for viscous fingering in compositional displacements for fully miscible cases. The theory adopts a fractional-flow formulation, rather than a dispersive formulation to describe average unstable displacement behavior. The width of the fingered zone is predicted to grow linearly with time. The study was only limited to homogenous media neglecting gravity and capillary forces.

Moissis *et al.* (1993) ^[25] studied the effect of gravity and of the structure of the porous medium on unstable miscible displacements using numerical simulations. Based on the study, fingers are generated due to heterogeneities of the porous medium. Results indicate that a displacement may be dominated by gravity or by viscous fingering or both mechanisms. When gravity tonguing is dominant, the results are early breakthrough and little oil recovery after breakthrough.

In miscible flooding project, viscous fingering is likely when the mobility ratio between oil and miscible gas is adverse. The more mobile gas fingers through the oil, leading to early solvent breakthrough. Alternating injection of water and miscible gas in a WAG process has been suggested as a way to reduce the impact of viscous fingering. Christie *et al.* (1993) ^[27] in their research presented the results of 2D and 3D high resolution simulation to assess the impact and importance of 3D effects in viscous fingering computations. The 3D computations give lower recovery and earlier breakthrough than the equivalent 2D calculations.

2.2 Gas Injection (EOR)

Secondary recovery stage reaches its limit when the injected fluid (water or gas) is produced in considerable amounts from the production wells and the production is no longer economical. The successive use of primary recovery and secondary recovery in an oil reservoir produced about 15% to 40% of the original oil in place.

Solvent flooding is a commonly used technology for EOR in hydrocarbon reservoirs, which aims at developing miscibility, thereby mobilizing the residual oil and enhancing the mobility of the hydrocarbon phase. ^[7] Two types of CO₂ displacement: ^[21]

a. Miscible CO₂ displacement:

Under suitable reservoir pressure and oil density conditions, injected CO₂ will mix thoroughly with the oil within the reservoir such that the interfacial tension between these two substances effectively disappears. Theoretically, all contacted oil can be recovered under miscible conditions. The suitable reservoir pressure and oil density conditions are generally deeper than 1,200 m with oil lighter than 22° API gravity.

b. Immiscible CO₂ displacement:

When reservoir pressure is too low and/or oil gravity too dense, the injected carbon dioxide remains physically distinct from the oil within the reservoir. However injected CO₂ can still improve oil recovery by causing the oil to swell, reducing the oil's density and improving mobility.

WAG is an EOR process where water and miscible solvent (gas) are alternately injected into a reservoir containing water and oil to provide better sweep efficiency. It helps to reduce the amount of viscous fingering in the reservoir by decreasing the apparent mobility contrast between the injected and displaced fluids hence improving sweep efficiency. ^[5] The fingering in a miscible flood, with only hydrocarbon flowing, can be modeled successfully using a Todd and Longstaff fractional flow. ^[5]

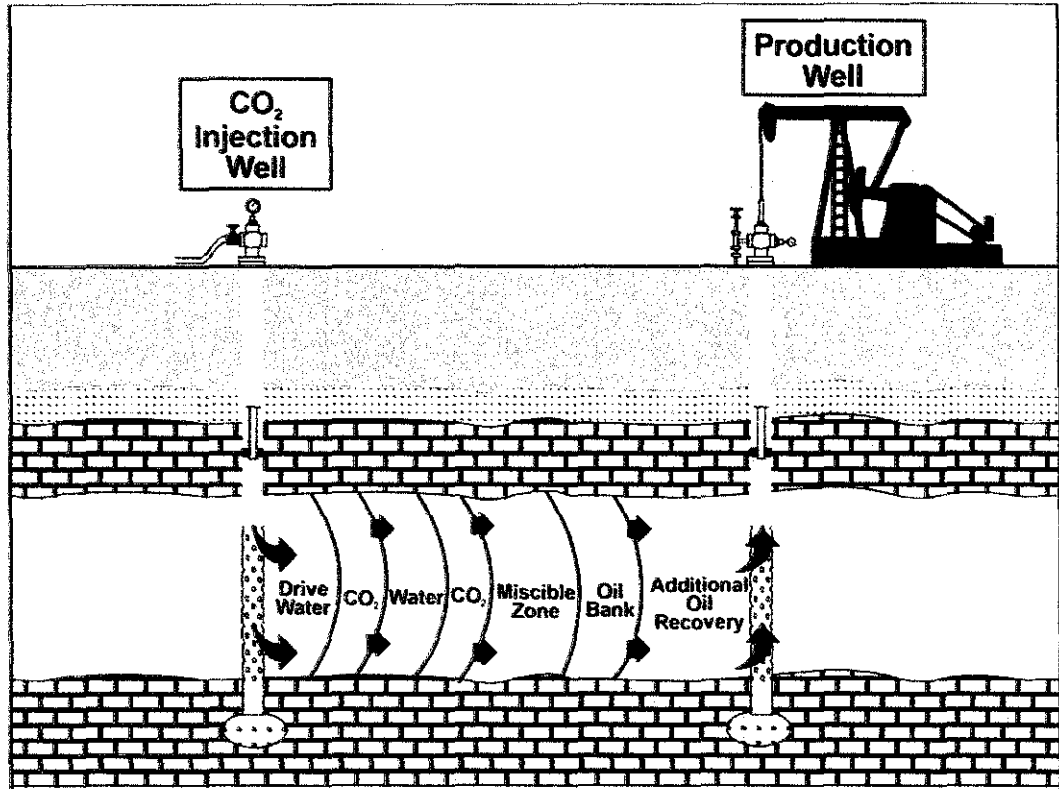


Figure 2 ^[21] : Illustration of WAG process

There is an optimum ratio of water to solvent injected (optimum WAG ratio), which minimizes the degree of fingering. ^[7] Optimum WAG ratio is the value of injected fractional flow of water, f_{inj} at which the solvent and water fronts move at the same speed. The estimates of the optimum WAG ratio that account for viscous fingering are lower than those that ignore viscous fingering effects. ^[9] This means that the number of pore volume injected (PVI) for complete oil recovery is minimized by injecting a higher solvent fraction than predicted by the Stalkup method.

$$W_R = \frac{f_{inj}}{1 - f_{inj}} \quad (1)$$

where

W_R = optimum WAG ratio

f_{inj} = fractional flow of water injected

The injected solvent and injected water naturally travel at different speeds – if much more solvent than water is injected, the solvent front moves ahead of the water and we see severe fingering of this solvent into the oil. If much more water than solvent is injected, the water moves ahead of the solvent. While this reduces the fingering, the recovery resembles that of a waterflood until the oil is contacted by the slow moving solvent front.

In a secondary WAG process, water and solvent are injected into a reservoir containing oil and connate water. The solvent displaces the oil in the hydrocarbon phase, but since the solvent (or gas) is less viscous than the oil, it fingers through the reservoir, resulting in early breakthrough. Water is more viscous than the solvent and so if water is injected together with solvent, the contrast in total mobility between the injected and displaced fluids is reduced thus there is less fingering. The physical origin of fingering is the contrast in total mobility between the injected and displaced fluids. ^[5]

Solvent flooding alone has high local displacement efficiency but the effectiveness of solvent injection is compromised by viscous fingering that leads to early water breakthrough and a slow rate of recovery. To counter the problem, WAG is introduced to control the mobility of the solvent by injecting alternating water and solvent slugs.

A numerical simulation study of EOR alternatives has been conducted for a reservoir by Todd *et al.* (1999) ^[13] The high asphaltene content of the crude, together with indication of plugging if precipitation is allowed to occur in the reservoir, has forced the maintenance of pressure by injection. The modeling work indicates significant sensitivity to both process and well configuration. Continuous gas injection predicted to

recover 0.03 to 0.09 oil initially-in-place (OIIP) more oil than water injection, and 1:1 WAG predicted to recover 0.06 to 0.10 OOIP more oil than continuous gas injection, depending on the well configuration.

2.3 Asphaltene

Asphaltene deposition causes serious problems in production operations, from the reservoir, through production tubing and in surface facilities. It also alters formation porosity, wettability and induces near-wellbore formation damage where permeability of the formation is reduced.

2.3.1 Definition

There are many definitions of asphaltene and the definitions are based on the asphaltene's solubility. Asphaltene recently defined by chemists as the part precipitated by addition of low-boiling paraffin solvent such as normal-pentane and benzene soluble fraction whether it is derived from carbonaceous sources such as petroleum, coal or oil shale.

For simplicity, asphaltene are the fraction of oil that is insoluble in n-heptane or n-pentane but soluble in benzene or toluene. Asphaltene are very complex molecules and they are the heaviest and most polar fractions found in crude oil.

2.3.2 Where asphaltene deposits are found? ^[15]

Asphaltene can be found:

- a. In surface facilities (pipelines and separators). Asphaltene deposition affects all the flow lines and it occurs regardless of the temperature conditions.
- b. In production tubing. Deposits were subsequently found in the tubing in which deposits form at corresponding to the bubble pressure of produced oil.
- c. Then the asphaltene deposit zone can migrate to bottomhole and well neighboring formation as reservoir depletion proceeds.

An important fact about asphaltene that often is overlooked is that they are deposited only after flocculation. ^[19] Avoiding asphaltene flocculation is a key to preventing asphaltene-induced formation damage. During flocculation, the asphaltene micelles rearrange, by losing resin molecules to form larger bodies.

Asphaltene deposition onto the rock surface causes wettability alteration from water-wet to oil-wet. Water-wet reservoir rocks permit more efficient oil production because of the favorable relative permeability to oil. ^[20] Inversely, oil flows with more difficulty through pore channels and throats that are more oil-wet than water-wet.

2.3.3 Relation between Asphaltene and Resin

Asphaltene precipitation is the result of instability of oil. The asphaltene are in nature stabilized by resins and maintained in the oil. The resins play an important role in the stability of petroleum and prevent separation of the asphaltene as separate phase. The resins will keep the asphaltene well dispersed in the oil and prevent them from precipitate, flocculate and lastly deposit on rock surface. Asphaltene precipitates due to several reasons like pressure drop, gas injection and change in oil composition and the asphaltene can cause problems to hydrocarbon production when it deposited in the reservoir and the wellbore. Higher rock heterogeneities would lead to higher asphaltene accumulation in a formation. ^[14]

The injected CO₂ when come in contacts with oil, can cause changes in the fluid behavior and equilibrium conditions and also alter the asphaltene-to-resin ratio of crude oil which results in asphaltene precipitation. ^[17] Precipitated asphaltene can either be flowing as suspended particles or deposited onto the rock surface causing formation damage. Asphaltene stability is factored by fluid composition, pressure and temperature.

As recognized by Boer *et al.* (1992) ^[6], light oil with small amount of asphaltene is more likely to cause problems during production than heavy oil even though heavy oil has larger amount of asphaltene. The explanation for this is the heavier oil contains plenty of intermediate components that are good asphaltene solvents whereas the light oil may consist mainly of lighter components which asphaltene have limited solubility.

Field and laboratory data confirm that asphaltene will precipitate more easily in light oil compared to heavy oil even though heavy oil have much higher asphaltene content compared to light oil. The Venezuelan Boscan crude with 17.2 wt% asphaltene was produced without asphaltene related problem, while the crude of Hassi-Messaoud in Algeria with only 0.15 wt% asphaltene has many asphaltene related production problems. ^[16]

2.3.4 Relation between CO₂ Concentration and Asphaltene Precipitation

Asphaltene precipitation increases with increasing concentration of injected CO₂ as reported by Alta'ee *et al.* (2010) ^[17]. The study was done on light oil sample at constant pressure and temperature. Moghadasi *et al.* (2006) ^[18] concluded from their results that the amount of asphaltene precipitation due to CO₂ injection is dependent on concentration of injected CO₂ gas and will rapidly increase when the gas concentration exceeds one critical value.

Based on the research by Srivastava *et al.* (1999) ^[26], static asphaltene precipitation tests indicated that the most important factor on which the asphaltene precipitation depended was CO₂ concentration. The effect of the presence of brine on asphaltene flocculation seemed to be negligible.

2.3.5 Asphaltene Precipitation, Flocculation and Deposition

Field conditions conducive for precipitation include normal depletion, acid stimulation, gas-lift operations, and miscible flooding. Precipitation of asphaltene depends on the composition of the oil and concentration of asphaltene in the oil.^[22] Precipitation occurs above the saturation pressure, reaches a maximum value at around the saturation pressure and decreases as pressure drops below the saturation pressure. As the light components come out of the solution, the solubility of asphaltene in the liquid phase increases.

Recent research has shown that asphaltene precipitation process is largely reversible. However, the time required for asphaltene to go back into solution may be longer than the time required for the original precipitates to form. Precipitated asphaltene that have not flocculated into larger particles may flow with the fluids without any harmful effects on production.

Flocculated asphaltene contributes to the formation of organic deposits causing problems such as formation damage, flow restriction due to partial plugging of the production string of pipelines and limitations in the crude oil and produced water treatment facilities due to the formation of stable emulsions. The precipitated asphaltene are fine particles that may form larger aggregates, which are large enough to be retained at small pore throats. Precipitated asphaltene can deposit onto the rock and cause plugging and wettability alteration.

CHAPTER 3

METHODOLOGY

3.1 Research Methodology

Below is the general work flow of this project:

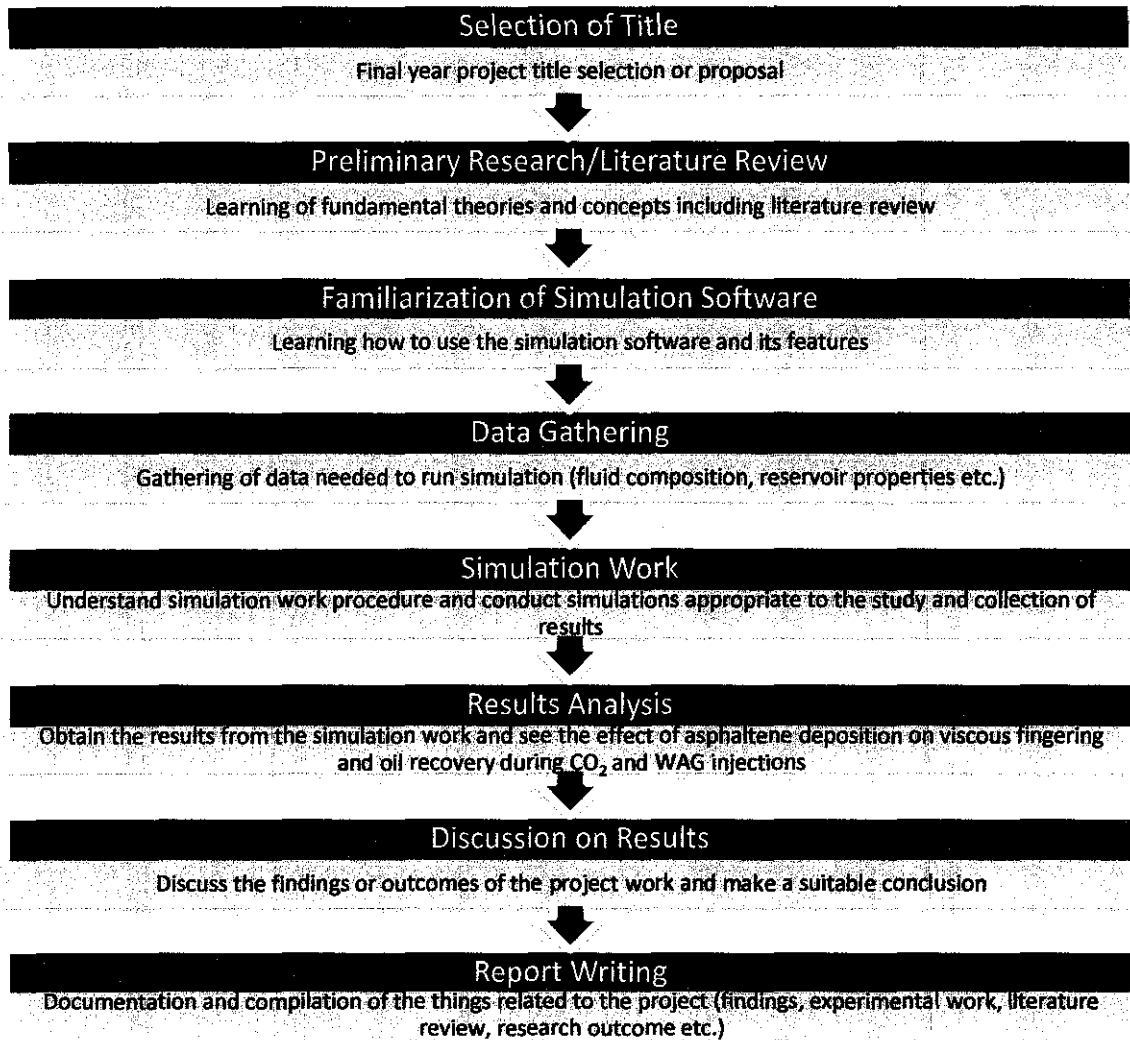


Figure 3: Research flowchart

3.1.1 Brief Explanation on Simulation Work

For the simulation work, it has been done using a set of software provided by CMG. The set of software are:

- a. GEM – is a full Equation of State compositional reservoir simulator with advanced features for modeling recovery processes where the fluid composition affects recovery.
- b. WINPROP – is used for modeling the phase behavior and properties of reservoir fluids.
- c. Builder – is an application used in the preparation of reservoir simulation models.
- d. Results 3D and Results Graph – are the applications used for interpreting simulation results.

Two types of formation have been modeled using Builder software in CMG. One formation is without presence of asphaltene deposition and another one with presence of asphaltene deposition. WINPROP was used to characterize the fluids that were used in the simulations. Tutorial for modeling asphaltene precipitation can be found in the manual that comes with the software.

The reservoir input data file needed for GEM simulation software was created using Builder. Then, data file from WINPROP (fluid characterization software) and Builder was imported to GEM. GEM simulated the flow of fluids injected and displaced during CO₂ and WAG injection process in the formation with and without asphaltene deposition.

Results 3D was used to see the fluid flow in a formation in 3D grid blocks while Results Graph was used to plot the necessary plots for this project. Size, shape and propagation of viscous fingering in all of the simulations have been observed and compared.

Simulation workflow:

1. Fluid characterization using WinProp.
 - Fluid data was taken from a paper.
2. Reservoir characterization, rock-fluid interaction properties, well configuration and initial reservoir conditions determination using Builder.
3. Running of data sets from Builder into GEM, compositional oil simulator.

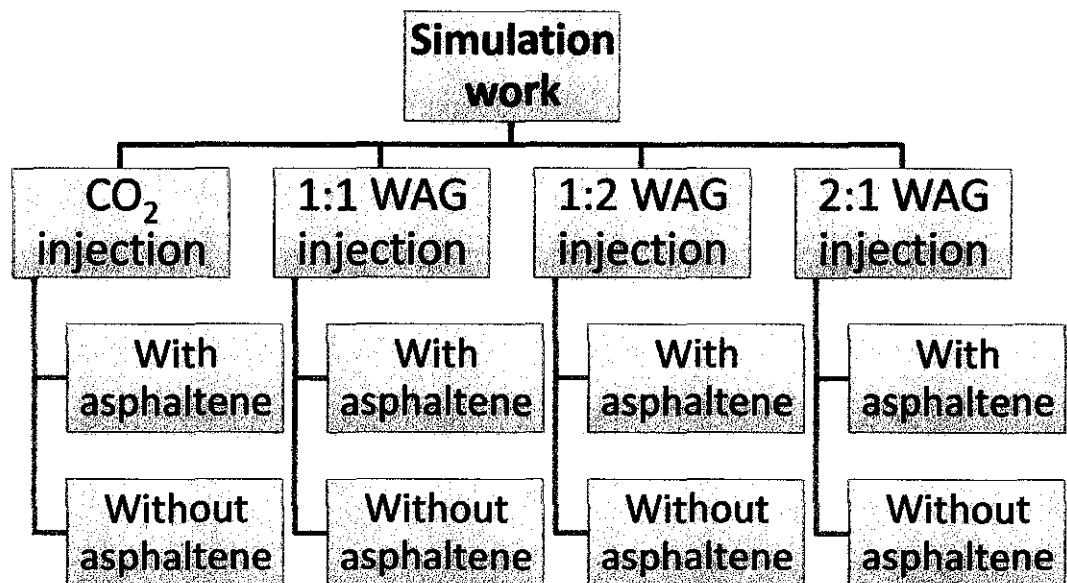


Figure 4: Main simulations for this project

4. Comparisons of viscous fingering and oil recovery between different types of simulation using Results 3D and Results Graph.

Below is an example of fluid analysis and asphaltene precipitation data taken from a journal paper by Burke, Hobbs and Kashou (1990) ^[22]:

| Component | Oil 1 |
|---|--------|
| Nitrogen | 0.57 |
| Carbon Dioxide | 2.46 |
| Methane | 36.37 |
| Ethane | 3.47 |
| Propane | 4.05 |
| i-Butane | 0.59 |
| n-Butane | 1.34 |
| i-Pentane | 0.74 |
| n-Pentane | 0.83 |
| Hexanes | 1.62 |
| Heptanes plus | 47.96 |
| Total | 100.00 |
| C ₇₊ molecular weight | 329 |
| C ₇₊ specific gravity | 0.9594 |
| Live oil molecular weight | 171.4 |
| Stock tank oil API gravity | 19.0 |
| Asphaltene content in stock tank oil, wt% | 16.8 |
| Reservoir temperature, °F | 212 |
| Saturation pressure, psia | 2950 |

Figure 5: Example of oil compositions and properties

3.2 Tools Required

The tool required for this study is simulation software provided by Computer Modelling Group Ltd. (CMG). The software has been used to simulate viscous fingering during CO₂ and WAG injection process in presence of asphaltene deposition.

3.3 Project’s Gantt Chart and Key Milestones

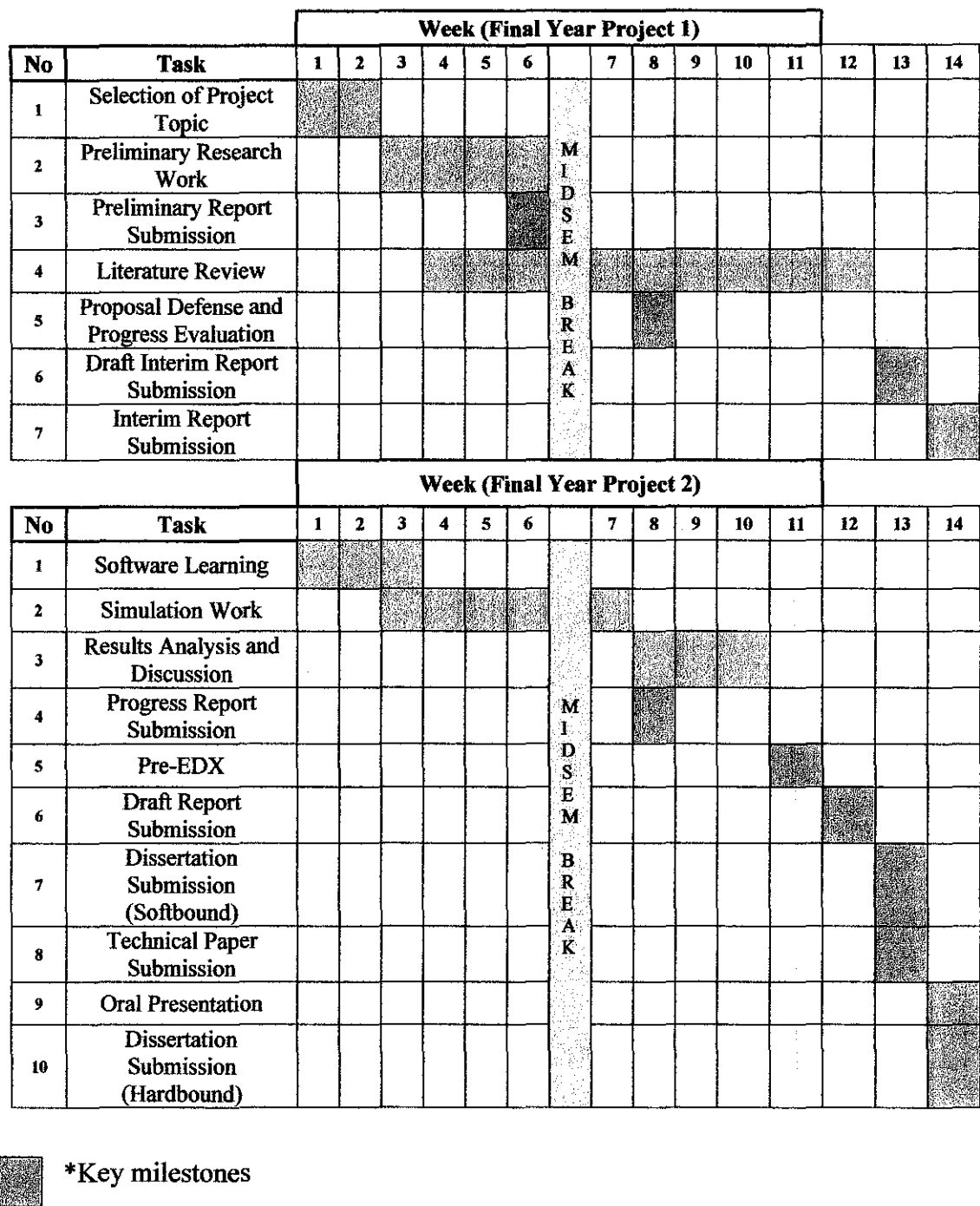


Figure 6: Gantt chart with key milestones

CHAPTER 4

RESULTS AND DISCUSSION

Viscous fingering effect simulation depends on grid size, injected solvent and produced oil viscosity and also the injection rate of solvent. In order to observe the fingering in detail, the number of grid block for the simulation must be high enough.

The valid license installed at the EOR Centre, Academic Block 15, UTP has limitations due to the type of license which is academic license. First, the maximum number of grid block that can be used is only 20,000. Second, the maximum number of processor core to be used for simulation is limited to only one. Because of the first limitation, all the simulations in this study were done using 17,600 grid blocks in 2D. 3D simulation needs higher amount of grid block in order to see viscous fingering in detail which is impossible due the limitation of academic license. Difference in initial viscosity of injected solvent and produced oil was kept high enough to see serious viscous fingering effect. CMG version 2009.10 has been used in this study.

4.1 Compositional Reservoir Simulation of Asphaltene Precipitation, Flocculation and Deposition using CMG GEM ^[31]

This section deals with the asphaltene precipitation, flocculation and deposition models implemented in CMG GEM for compositional simulation of asphaltene precipitation and plugging in hydrocarbon formations.

4.1.1 Asphaltene Precipitation Model

The precipitated asphaltene is modeled as a pure solid. The pure solid is described by splitting the heaviest pseudo component in the oil characterization into a non-precipitating component and a precipitating component. The two components have identical critical properties and acentric factors, but different interaction parameters with the light components in the system. The precipitating component may be considered to include both asphaltene and resin molecules.

The component fugacities in the oil and gas phases are calculated from the Peng-Robinson EOS. The solid fugacity, f_{s1} , is given by:

$$\ln f_{s_1} = \ln f_{s_1}^* + \frac{v_{s_1} (p - p^*)}{R T} \quad (2)$$

where

f_{s_1} = fugacity of solid s_1 , kPa

$f_{s_1}^*$ = reference solid fugacity, kPa

v_{s_1} = solid molar volume, m³/mol

p = pressure, kPa

p^* = reference pressure, kPa

R = universal gas constant

T = temperature, K

As the formation of the precipitated solid is governed solely by thermodynamic equilibrium conditions, it will exhibit complete thermodynamic reversibility that is any precipitated solid s_1 will go back into solution when the system is returned to a state outside the asphaltene precipitation envelope.

4.1.2 Asphaltene Flocculation Model

Asphaltene flocculation refers to the flocculation of precipitated asphaltene particles into larger aggregates. Irreversibility of solid precipitates is modeled by allowing solid s_1 to be transformed via a simple reversible chemical reaction into another solid, s_2 . This can be viewed as the flocculation of smaller asphaltene particles into larger aggregates.



Solid s_2 can go back into solution first by becoming solid s_1 through the reverse reaction. The solid then dissolving into the oil phase through thermodynamic equilibrium.

The reaction rate for the formation of solid s_2 is:

$$r = k_{12} C_{s_1,o} - k_{21} C_{s_2,o} \quad (4)$$

where

- k_{12} = forward rate of formation of solid s_2 from s_1 [day^{-1}]
- k_{21} = reverse rate of formation of solid s_1 from s_2 [day^{-1}]
- r = reaction rate [$\text{mol}/(\text{m}^3 \text{ day})$]
- $C_{s_1,o}$ = concentration of suspended solid s_1 in oil phase [mol/m^3]
- $C_{s_2,o}$ = concentration of suspended solid s_2 in oil phase [mol/m^3]

If k_{21} is zero, the reaction is reversible and solid s_2 will not go back into the solution. If $k_{21} < k_{12}$, the precipitation of solid s_2 is reversible. The reversal may take a long time to complete. The above reaction allows the modeling of irreversible precipitation or a slow redissolution of precipitated asphaltene.

4.1.3 Asphaltene Deposition Model

Wang and Civan (2001) ^[28] presented an equation relating asphaltene deposition rate to the primary physical deposition processes including solid adsorption, pore throat plugging and re-entrainment. The model has been implemented in CMG GEM. Based on the implementation, only solid s_2 (flocculated particles) is considered to deposit.

This implies that the small asphaltene precipitate particles are more likely to flow with the oil phase, while the larger aggregates are more likely to deposit on the reservoir rock. The deposition rate equation is:

$$\frac{V_{s_2}^{n+1} - V_{s_2}^n}{\Delta t} - \alpha C_{s_2}^{n+1} \phi^{n+1} + \beta V_{s_2}^{n+1} (v_o^n - v_{cr,o}) - \gamma u_o^n C_{s_2}^{n+1} = 0 \quad (5)$$

where

| | | |
|------------|---|---|
| V_{s_2} | = | volume of deposited solid s_2 per gridblock volume |
| C_{s_2} | = | volumetric concentration of flowing solid s_2 per volume of oil |
| v_o | = | oil phase interstitial velocity |
| $v_{cr,o}$ | = | critical oil phase interstitial velocity |
| u_o | = | oil phase Darcy velocity |
| α | = | surface deposition rate coefficient |
| β | = | entrainment rate coefficient |
| γ | = | pore throat plugging rate coefficient |

The surface deposition rate coefficient, α is a positive constant and is dependent on the rock type. The pore-throat plugging coefficient is set to zero if the average pore throat diameter is larger than some critical value. If it is smaller, the coefficient is calculated as:

$$\gamma = \gamma_i \left(1 + \sigma V_{s_2} \right) \quad (6)$$

where

| | | |
|------------|---|---|
| γ_i | = | instantaneous pore throat plugging rate coefficient |
| σ | = | snowball-effect deposition constant |

4.1.4 Permeability Resistance Factor in CMG GEM

In a study by Reis and Acock (1994) ^[29] on inorganic solid deposition in sandstone cores, they concluded that exponential and power-law models may be used for deposition-induced permeability reductions of up to about 80% provided that proper empirical constants are used. The power-law model equation is:

$$k = c \phi^b \quad (7)$$

where

k = absolute permeability, md
 ϕ = porosity

Once the solid phase has adsorbed on the reservoir rock, partial plugging of the formation is expected. GEM uses a simple model for these phenomena based on a resistance factor. The power law is used to derive an equation for the resistance factor, R_f which relates the original permeability k_0 to the instantaneous permeability k as a function of the ratio of the original porosity to the instantaneous porosity:

$$R_f = \frac{k_0}{k} = \left(\frac{\phi_0}{\phi} \right)^b \quad (8)$$

where

R_f = permeability resistance factor
 k_0 = original permeability
 k = instantaneous permeability
 ϕ_0 = original porosity
 ϕ = instantaneous porosity

The instantaneous porosity equation is:

$$\phi = \phi_0 - V_{s_2} \quad (9)$$

where

ϕ_0 = original porosity
 ϕ = instantaneous porosity
 V_{s_2} = volume of deposited solid s_2 per gridblock volume

The resistance factor is divided into each of the gas, oil and aqueous phase mobilities, thereby reducing the volumetric flow rates for all flowing phases in order to account for the reduced permeability effect due to asphaltene deposition. In CMG GEM, the same factor is applied to oil, gas and water phases.

4.2 Asphaltenic Oil Modeling using WinProp

This section covers the results and discussion on the asphaltene precipitation modeling work that has been done for this project. In order to model and simulate asphaltene flocculation and deposition in the formation using GEM, asphaltene precipitation must be modeled first using fluid modeling software, WinProp. The fluid model from WinProp is then imported to Builder. GEM, a compositional oil simulator uses the data files created by Builder.

Asphaltene precipitation of Oil 1 (heavy oil) and Oil 2 (light oil) was modeled. Initial test simulations were using Oil 1 and main simulations for this project were using Oil 2. Fluid analysis data for Oil 1 and Oil 2 were taken from Burke, Hobbs and Kashou, "Measurement and Modeling of Asphaltene Precipitation", Journal of Petroleum Technology, November 1990, pp. 1440-1446.

The crucial step in modeling asphaltene precipitation is the characterization of the solid forming components, both in solution and in the solid phase. It was found that by splitting the heaviest components into two components, a non-precipitating and a precipitating fraction, good quantitative match with experimental data was obtained.

Table 1: Oil 1 (heavy oil) and Oil 2 (light oil) properties ^[22]

| Component | Oil | |
|---|-------------|-------------|
| | 1 | 2 |
| Nitrogen | 0.57 | 0.25 |
| CO ₂ | 2.46 | 2.03 |
| Methane | 36.37 | 32.44 |
| Ethane | 3.47 | 15.50 |
| Propane | 4.05 | 6.54 |
| i-Butane | 0.59 | 0.81 |
| n-Butane | 1.34 | 3.20 |
| i-Pentane | 0.74 | 1.15 |
| n-Pentane | 0.83 | 2.13 |
| Hexanes | 1.62 | 2.46 |
| Hexanes plus | 47.96 | 33.49 |
| Total | 100 | 100 |
| C ₇₊ molecular weight | 329 | 223 |
| C ₇₊ specific gravity | 0.9594 | 0.8423 |
| Live-oil molecular weight | 171.4 | 95.2 |
| API gravity, stock tank oil | 19.0 | 38.8 |
| Asphaltene content in stock tank oil, wt% | 16.8 | 1.7 |
| Reservoir temperature, °F | 212 | 234 |
| Saturation pressure, psia | 2950 | 2492 |

Table 2: Modeled fluid composition for Oil 1 and Oil 2 in WinProp

| OIL 1 | | | OIL 2 | | |
|-----------|--------|-----------|-----------|----------|-----------|
| Component | Mole % | MW | Component | Mole % | MW |
| CO2 | 2.46 | 44.01 | CO2 | 2.03 | 44.01 |
| N2 | 0.57 | 28.013 | N2 | 0.25 | 28.013 |
| C1 | 36.37 | 16.043 | C1 | 32.44 | 16.043 |
| C2 | 3.47 | 30.07 | C2 | 15.5 | 30.07 |
| C3 | 4.05 | 44.097 | C3 | 6.54 | 44.097 |
| i-C4 | 0.59 | 58.124 | i-C4 | 0.81 | 58.124 |
| n-C4 | 1.34 | 58.124 | n-C4 | 3.2 | 58.124 |
| i-C5 | 0.74 | 72.151 | i-C5 | 1.15 | 72.151 |
| n-C5 | 0.83 | 72.151 | n-C5 | 2.13 | 72.151 |
| FC6 | 1.62 | 86.000 | FC6 | 2.46 | 86.000 |
| C7-C15 | 19.66 | 147.27238 | C7-C12 | 15.6754 | 127.35883 |
| C16-C25 | 12.55 | 279.23117 | C13-C17 | 7.28706 | 205.83943 |
| C26-C30 | 4.00 | 389.52739 | C18-C23 | 4.92755 | 281.64483 |
| C31A+ | 7.42 | 665.624 | C24A+ | 5.24928 | 461.442 |
| C31B+ | 4.32 | 665.624 | C24B+ | 0.350756 | 461.442 |

Based on Table 2, as mentioned earlier, the precipitated asphaltene is modeled as a pure solid. The pure solid is described by splitting the heaviest pseudo component in the oil characterization into a non-precipitating component and a precipitating component. The non-precipitating component is the C31A+ and C24A+ fraction while the precipitating component is the C31B+ and C24B+ fraction. The A and B components have identical critical properties and acentric factors, but different interaction parameters with the light components in the system. The B component has much higher interaction parameters with the light components compared to the A component.

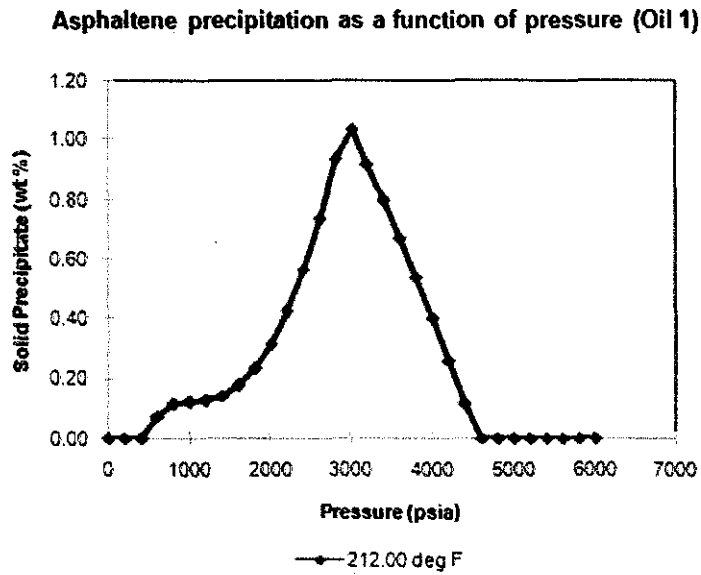


Figure 7: Modeled asphaltene precipitation as a function of pressure for Oil 1

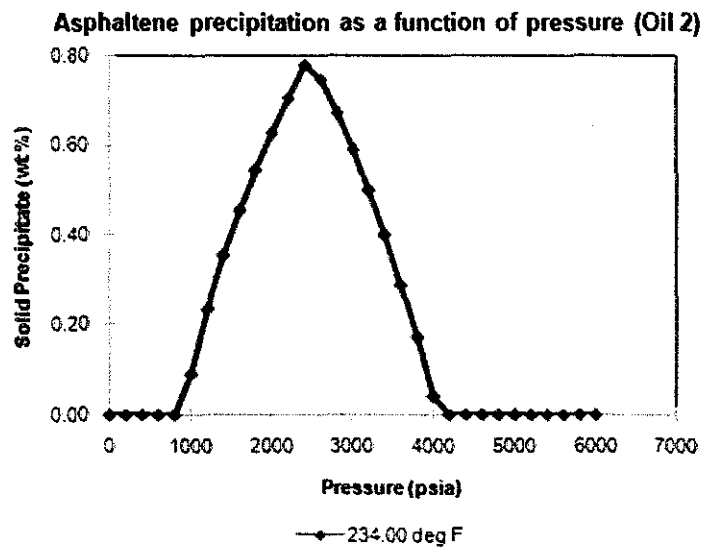


Figure 8: Modeled asphaltene precipitation as a function of pressure for Oil 2

Based on Figure 7 and Figure 8, asphaltene onset pressure can be known for each oil type. Oil 1 has asphaltene onset pressure of 4600 psia while Oil 2 has asphaltene onset pressure of 4200 psia. The asphaltene precipitation models were accurately modeled using WinProp since the maximum amount of asphaltene precipitation for each type of oil occurs around their saturation pressure. Precipitation occurs below the asphaltene onset pressure, reaches a maximum value at around the saturation pressure and decreases as pressure drops below the saturation pressure. ^[30] ^[31]

4.3 Main Simulation of Viscous Fingering using GEM

This section covers the results of the viscous fingering simulations that have been done to satisfy the objective of this project.

Figure 4 in Methodology Section shows the main simulations that were run for this study. Additional simulations will also be discussed in this report but they are not very significant in this study. All the main simulations were run in a heterogeneous formation since early simulations using homogeneous only resulted in the formation of gravity tongue and no viscous fingering occurred. Viscous fingering was simulated in two types of formation; formation without asphaltene deposition and formation with asphaltene deposition during CO₂ injection and WAG injection.

As mentioned earlier, asphaltene precipitation modeling was done using WinProp. However, WinProp does not have the ability to model asphaltene flocculation and deposition. This means that precipitated asphaltene will not flocculate and deposit in the formation. In order to model asphaltene flocculation and deposition, specific keywords have to be put in GEM data files manually.

In general, viscous fingering was only observed in the simulations where the formation is heterogeneous. No viscous fingering was observed in homogeneous formation. In homogeneous formation, only gravity tongue was observed which was due to gravity effect. Early test simulations were conducted using low resolution grid blocks and viscous fingering can be observed but in less detail. By refining the grid blocks used for the simulations, viscous fingering can be observed in more detail.

Based on a research by Tchelepi & Orr. Jr. (1993) ^[10], they presented various comparisons of viscous fingering between several cases at the same amount of pore volume injected by gas (PVI). In order to compare viscous fingering between two cases accurately, the comparison must be done at the same amount of PVI so in this project,

the results in terms of viscous fingering are compared at the same PVI. The comparison has been done in terms of oil saturation in the formation.

Simulations of viscous fingering were run during CO₂ injection and WAG injection. In order to simulate the alternating injection of water and gas during WAG, two injectors must be specified at the same perforation in Builder. Below is the 3D view of the formation used:



Figure 9: 80 x 1 x 20 grid block configuration (Length/height = 16)

Injectors is specified on the left end of the formation while producer is specified on the right end. The formation is 800 ft in length, 10 ft in width and 50 ft in thickness and has been modeled with 17,600 grid blocks which include refinement of grid block in the z-direction in order to see viscous fingering in detail. Reservoir has been modeled as heterogeneous in order to see severe viscous fingering effect. The permeability distribution for the heterogeneous formation is attached in appendix section.

Table 3: Reservoir properties calculated by GEM

| | |
|--|---------------------------|
| Total bulk reservoir volume, res ft ³ | 4.0 x 10 ⁵ |
| Total pore volume, res ft ³ | 8.07148 x 10 ⁴ |
| Total hydrocarbon pore volume, res ft ³ | 6.45718 x 10 ⁴ |
| Original oil in place, std bbl | 7.48775 x 10 ³ |

For every types of injection method, simulation results in terms of viscous fingering were compared at the same PVI and time for the two types of formation (with asphaltene deposition and without asphaltene deposition). The base case for each injection is the one without asphaltene deposition. The reason of comparing the viscous fingering in the two types of formation at the same PVI is to see whether asphaltene deposition affects the shape and size of the viscous fingering. Viscous fingering is compared between the two types of formation at the same time to see the effect of asphaltene deposition on the speed of propagation of viscous fingering.

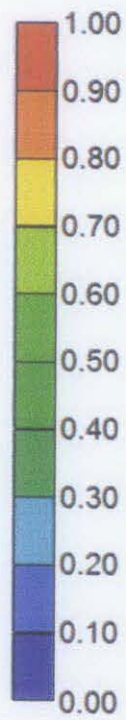


Figure 10: Colour scale used in showing CO₂ distribution across formation

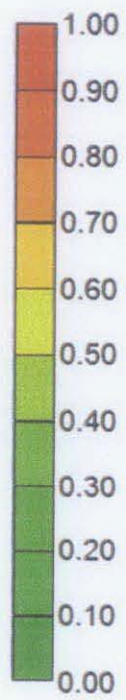


Figure 11: Colour scale used in showing oil saturation across formation

Table 4: General simulation properties

| RESERVOIR | |
|--|--|
| Reservoir pressure | 3000 psia |
| Reservoir temperature | 234°F |
| Average permeability in X, Y and Z directions | X=172.5 md, Y=172.5 md, Z=19.75 md |
| Porosity | 0.20 |
| Oil saturation | 0.80 |
| Connate water saturation | 0.20 |
| Grid block dimension (X x Y x Z) | 80 x 1 x 20 with refinement = 11 in z-axis (X=800 ft, Y=10 ft, Z=50 ft) |
| Initial condition | Oil and water only present. Reservoir is undersaturated. |
| OIL 2 | |
| API gravity | 38.8 |
| Saturation pressure | 2492 psia |
| WELL | |
| CO₂ injector constraint | Maximum bottomhole pressure = 3000 psia |
| Water injector constraint | Maximum bottomhole pressure = 3000 psia |
| Producer constraint | Minimum bottomhole pressure = 2500 psia |
| Injector fluid | Water and CO ₂ |
| EOR process | CO ₂ and WAG injection (1:1, 1:2 and 2:1 WAG scheme) |
| Perforation | 50 ft (all layers) |

4.3.1 Viscous Fingering Simulation during CO₂ Injection

Below are the results:

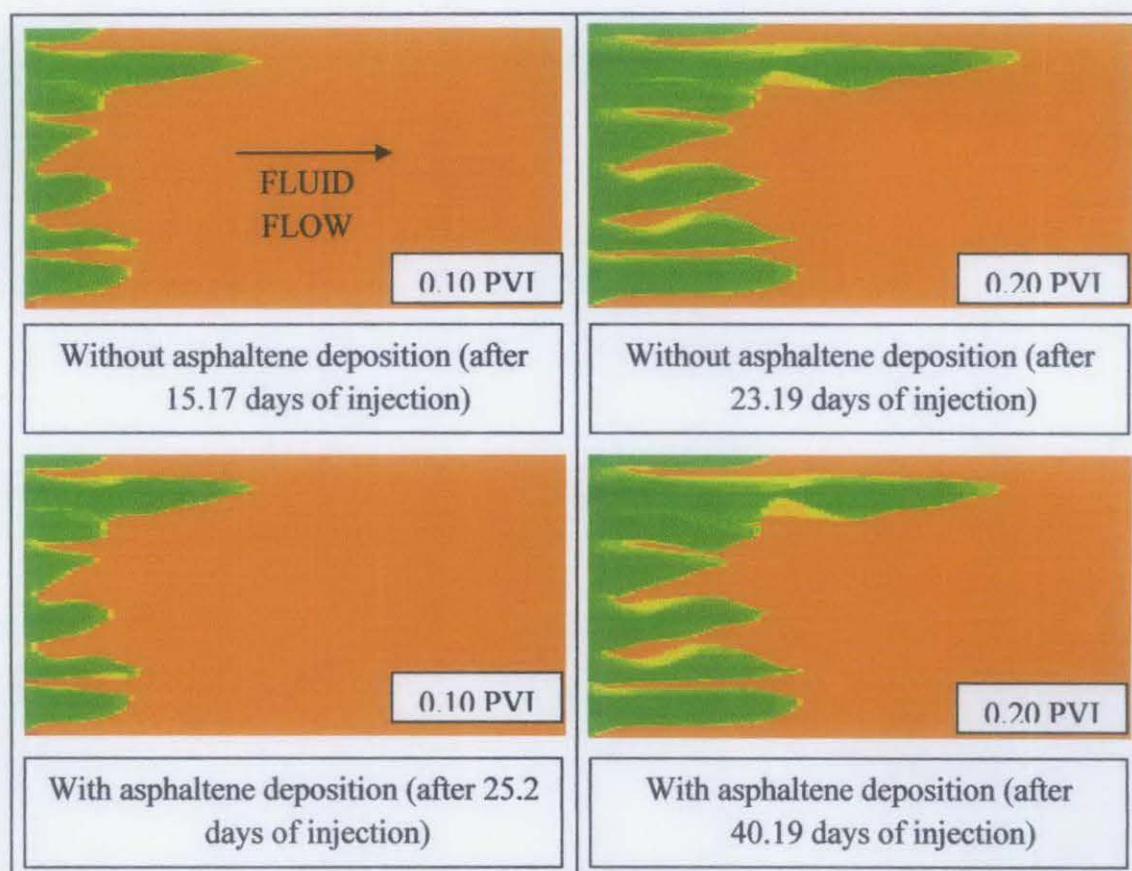


Figure 12: Oil saturation at 0.10 PVI (left) and 0.20 PVI (right)

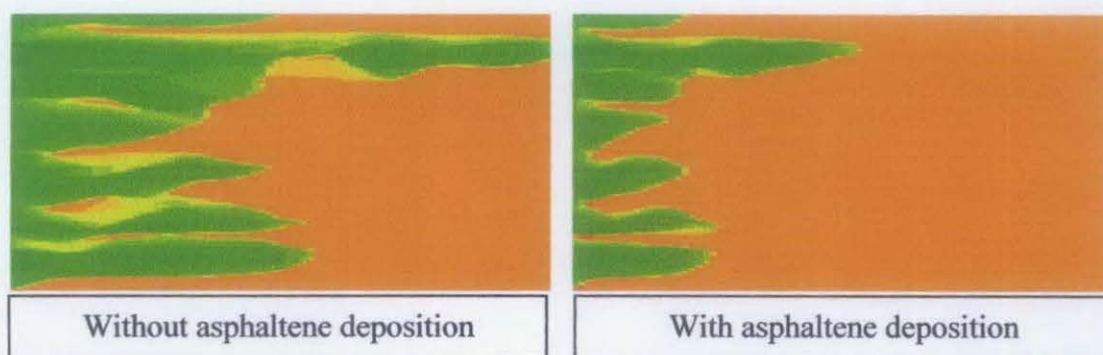


Figure 13: Oil saturation after 30 days of CO₂ injection

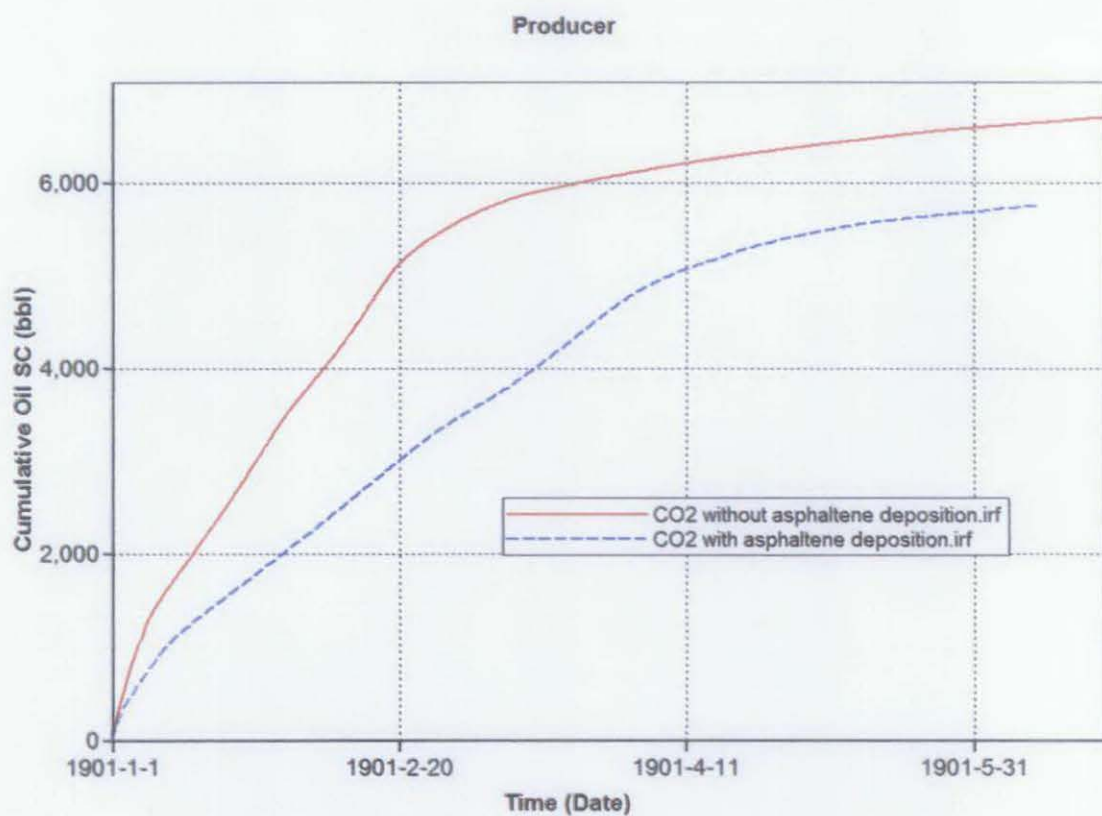


Figure 14: Cumulative oil produced, bbl vs. time

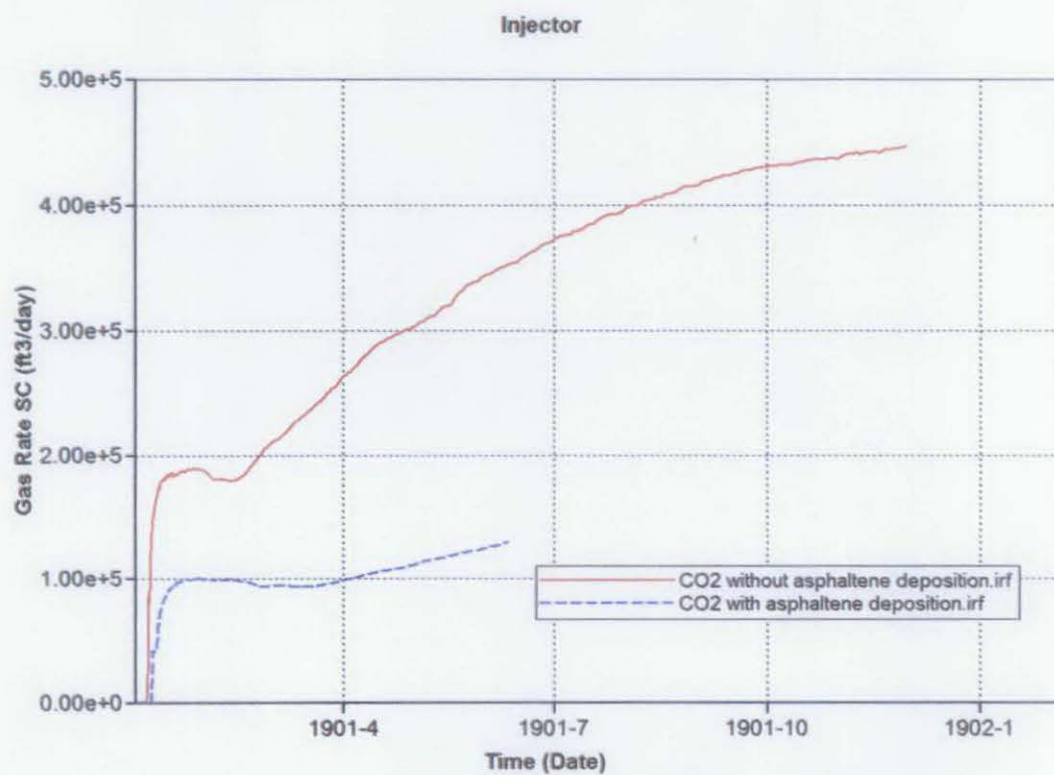


Figure 15: Injector gas rate, ft³/day vs. time

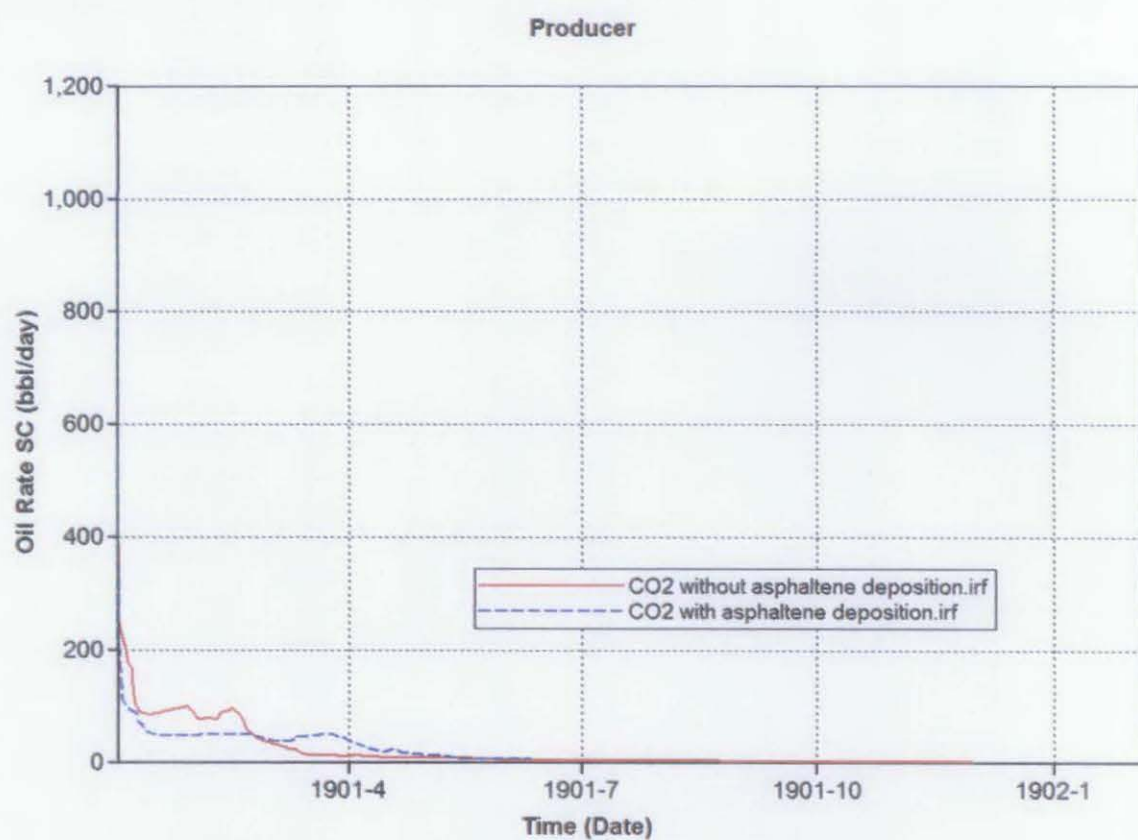


Figure 16: Producer oil rate, bbl/day vs. time

4.3.2 Viscous Fingering Simulation during 1:1 WAG Injection

In 1:1 WAG injection scheme, it started with 10 days of water injection followed by 10 days of CO₂ injection and then followed again by 10 days of water injection. The cycle keeps repeating until the simulation stops.

Below are the results:

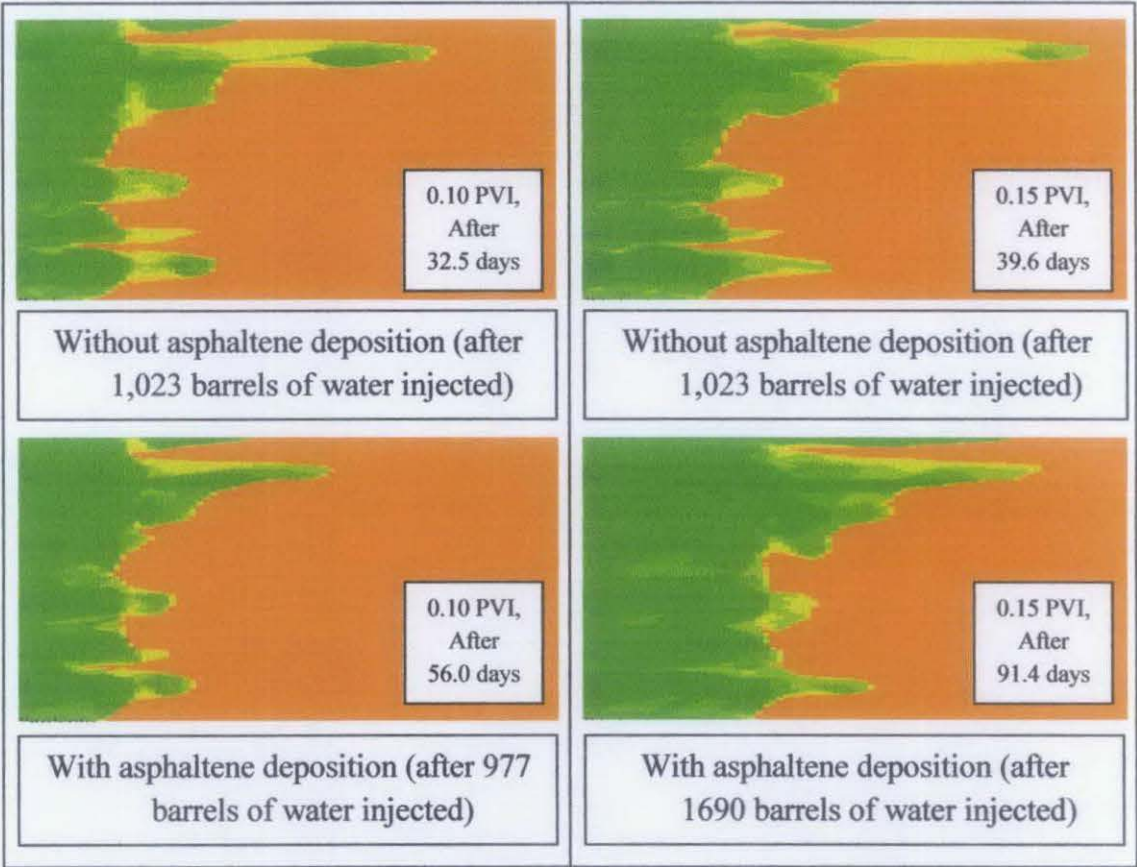


Figure 17: Oil saturation at 0.10 PVI (left) and 0.15 PVI (right)

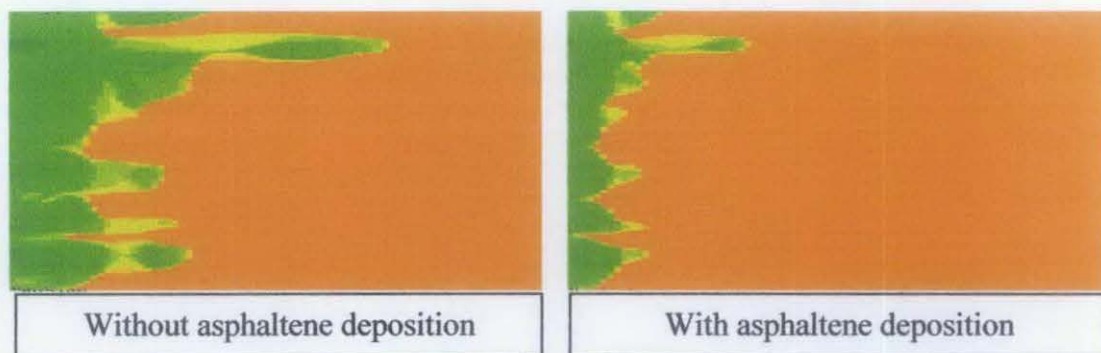


Figure 18: Oil saturation after 30 days of 1:1 WAG injection

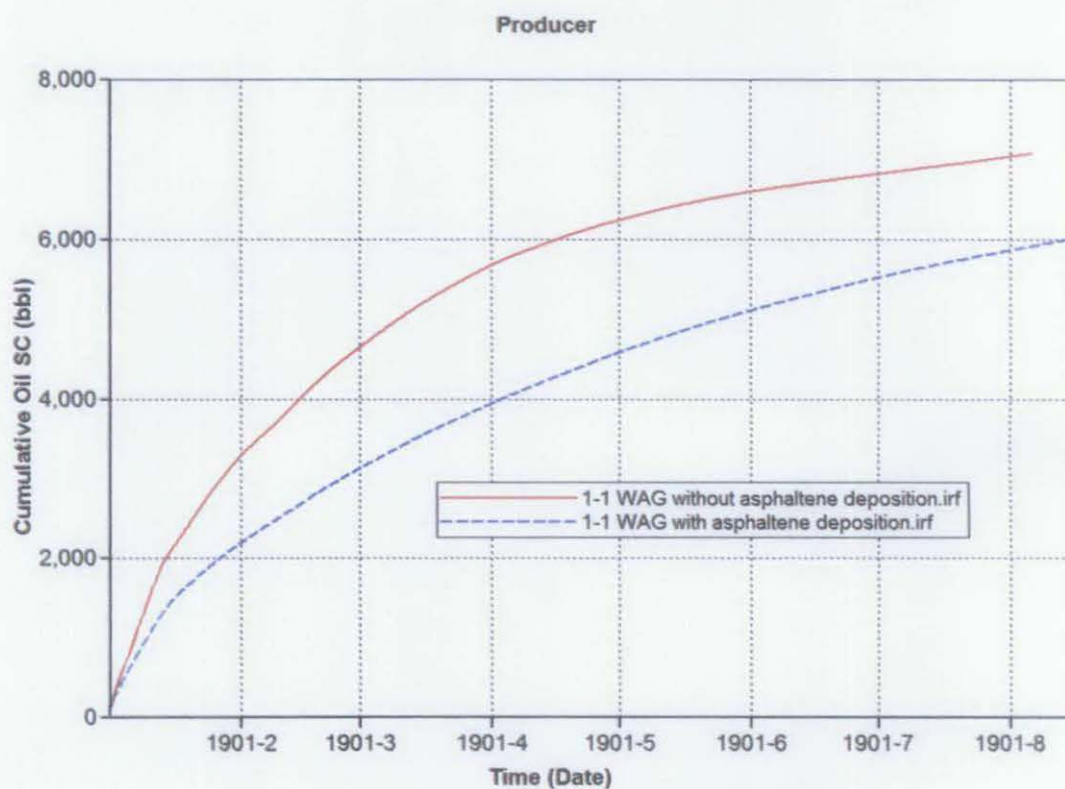


Figure 19: Cumulative oil produced, bbl vs. time

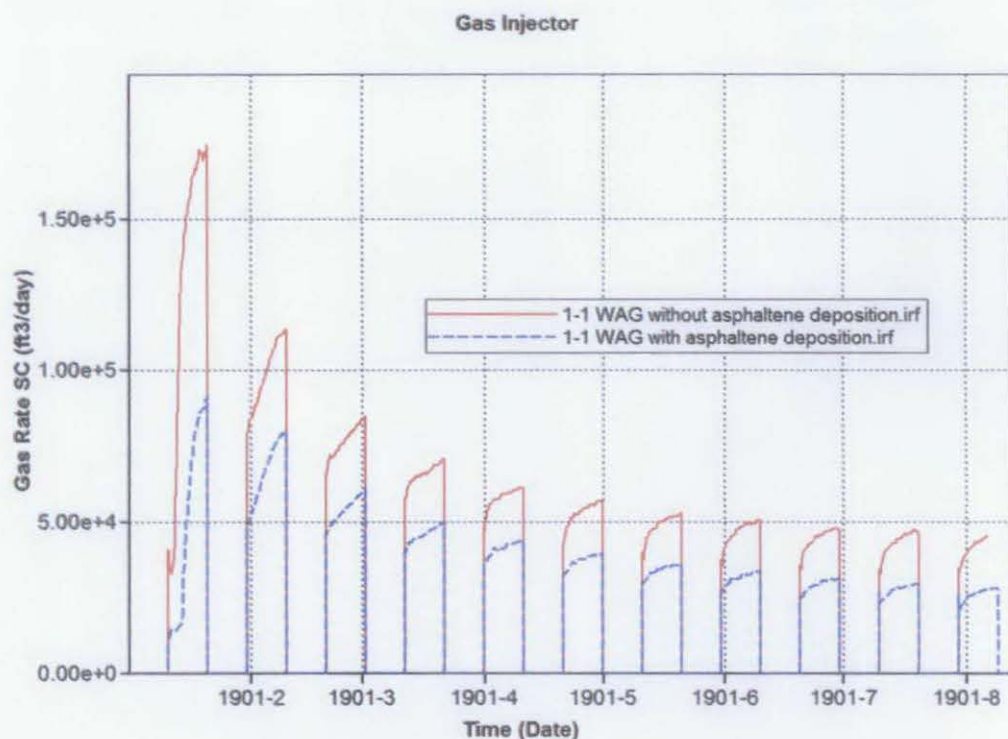


Figure 20: Injector gas rate, ft³/day vs. time

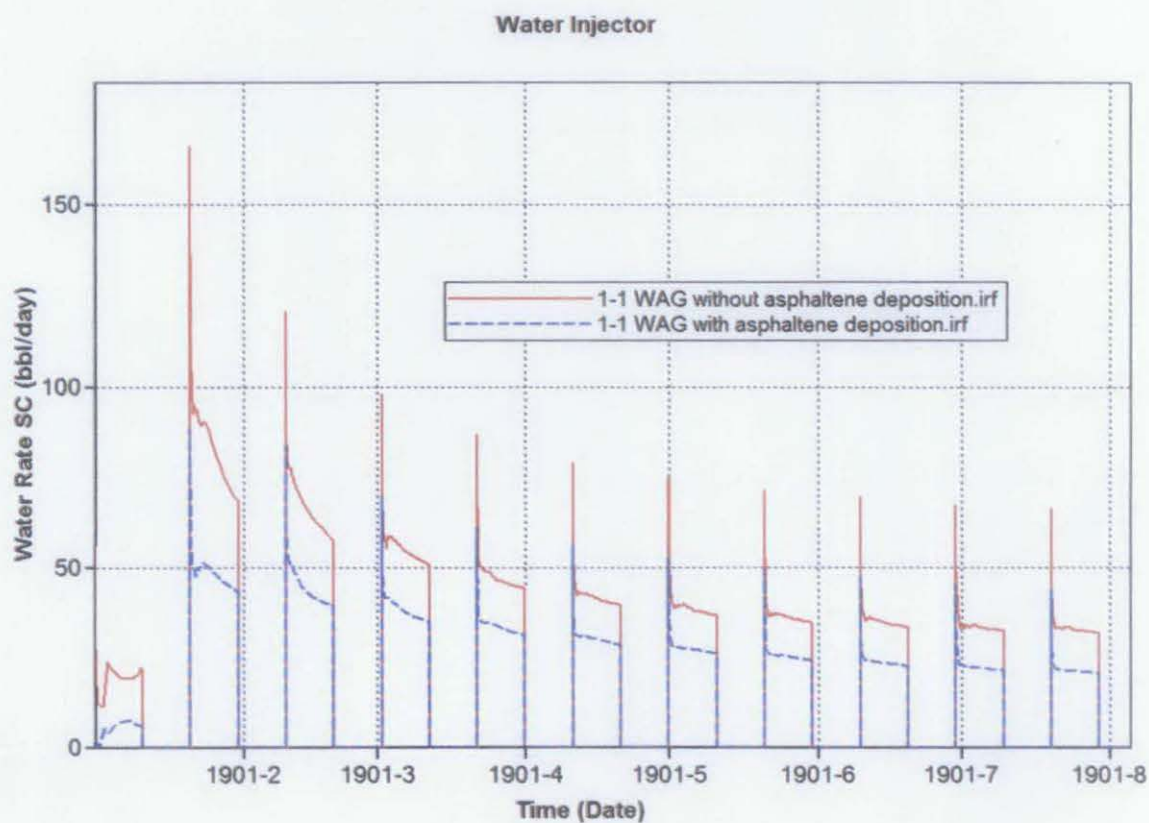


Figure 21: Injector water rate, bbl/day vs. time

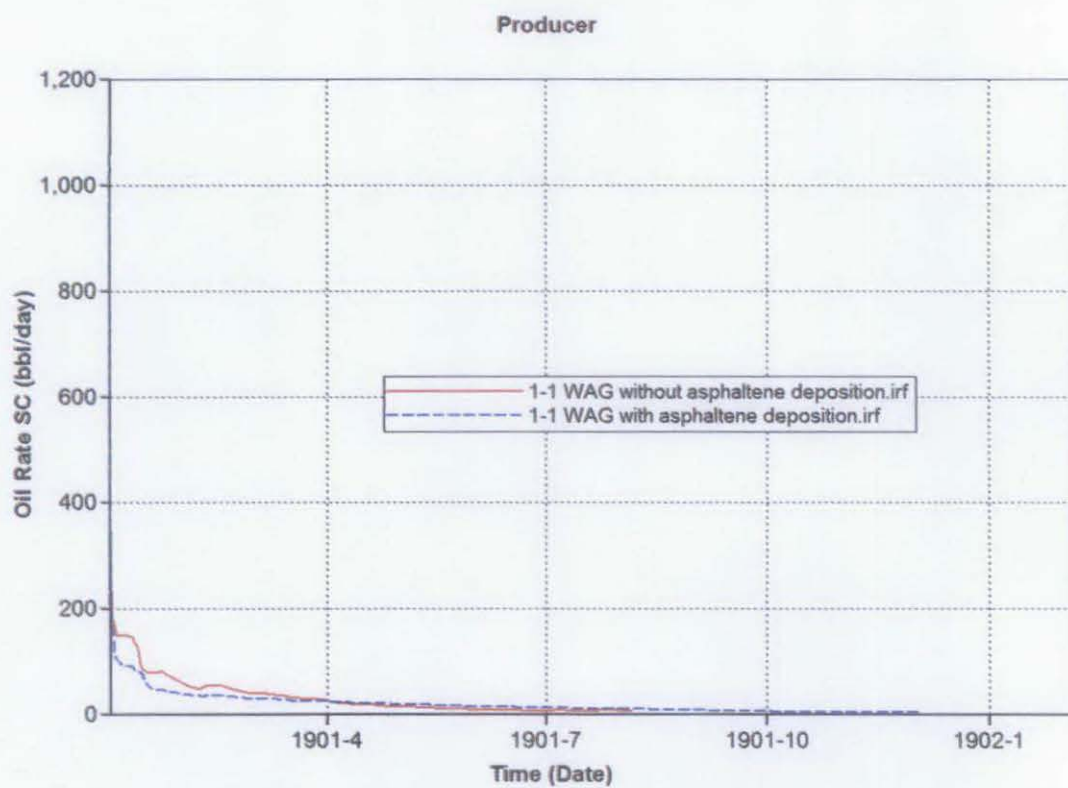


Figure 22: Producer oil rate, bbl/day vs. time

4.3.3 Viscous Fingering Simulation during 1:2 WAG Injection

In 1:2 WAG injection scheme, it started with 10 days of water injection followed by 20 days of CO₂ injection and then followed again by 10 days of water injection. The cycle keeps repeating until the simulation stops.

Below are the results:

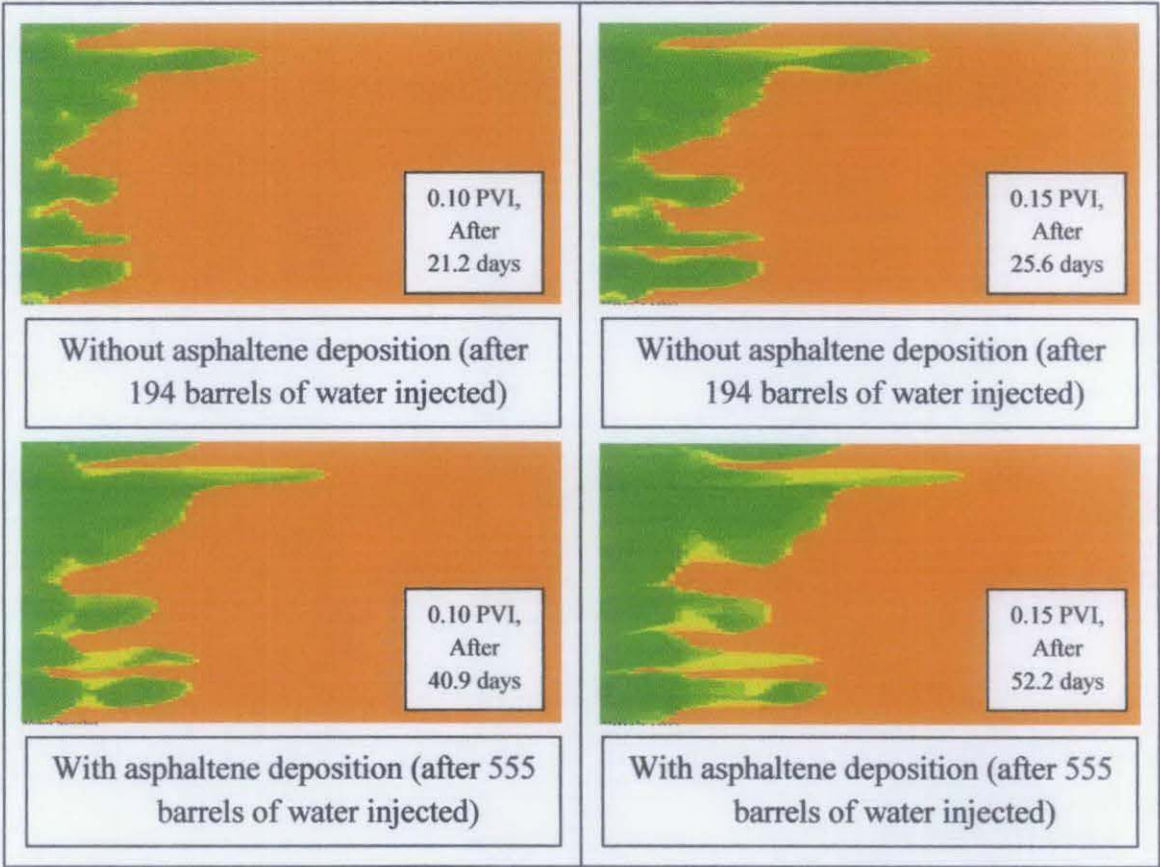


Figure 23: Oil saturation at 0.10 PVI (left) and 0.15 PVI (right)

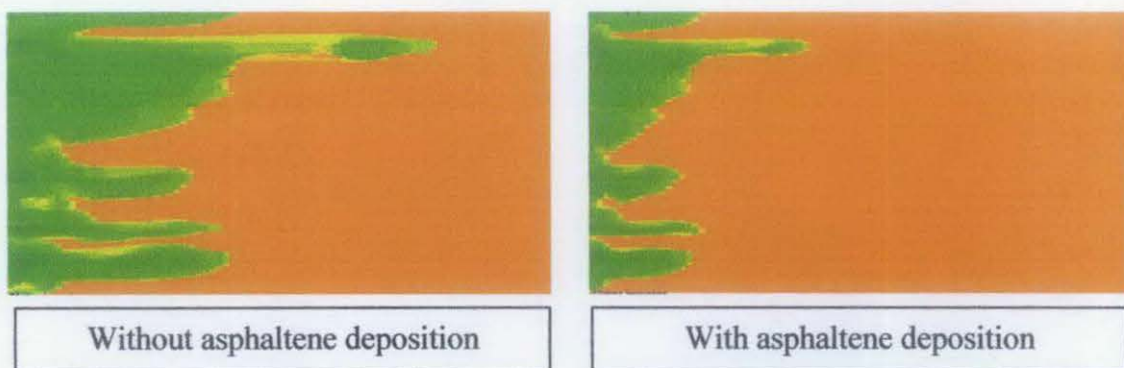


Figure 24: Oil saturation after 30 days of 1:2 WAG injection

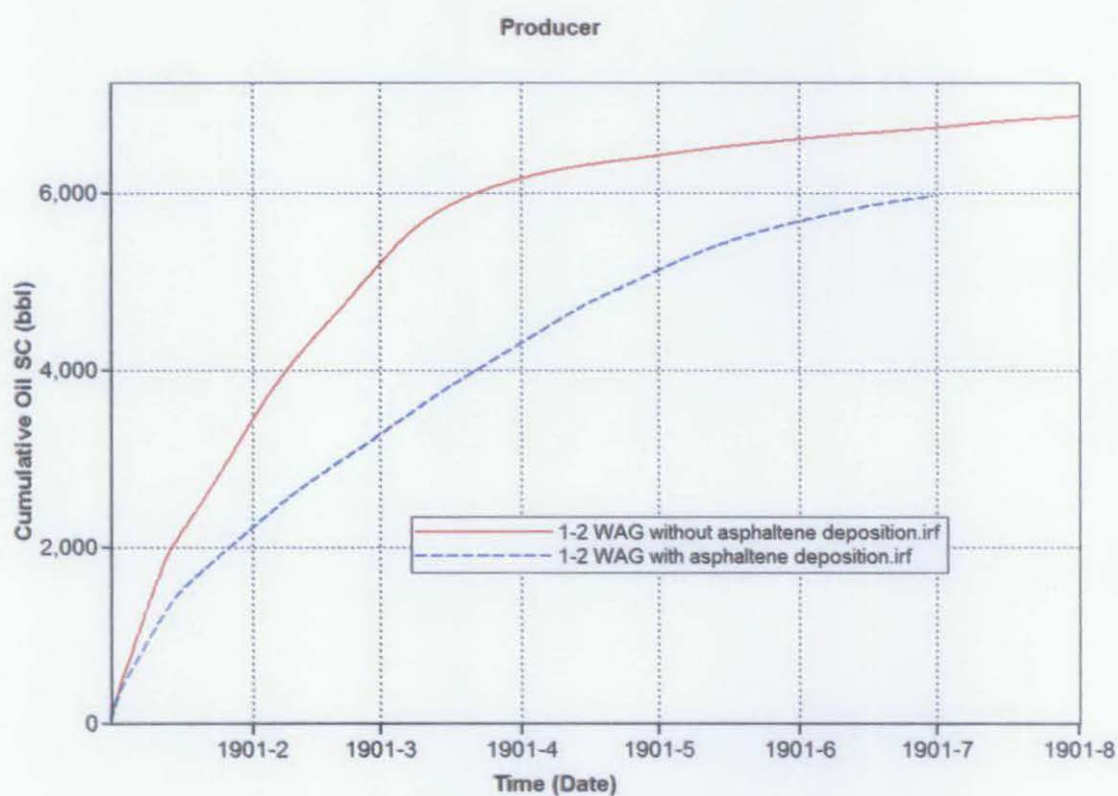


Figure 25: Cumulative oil produced, bbl vs. time

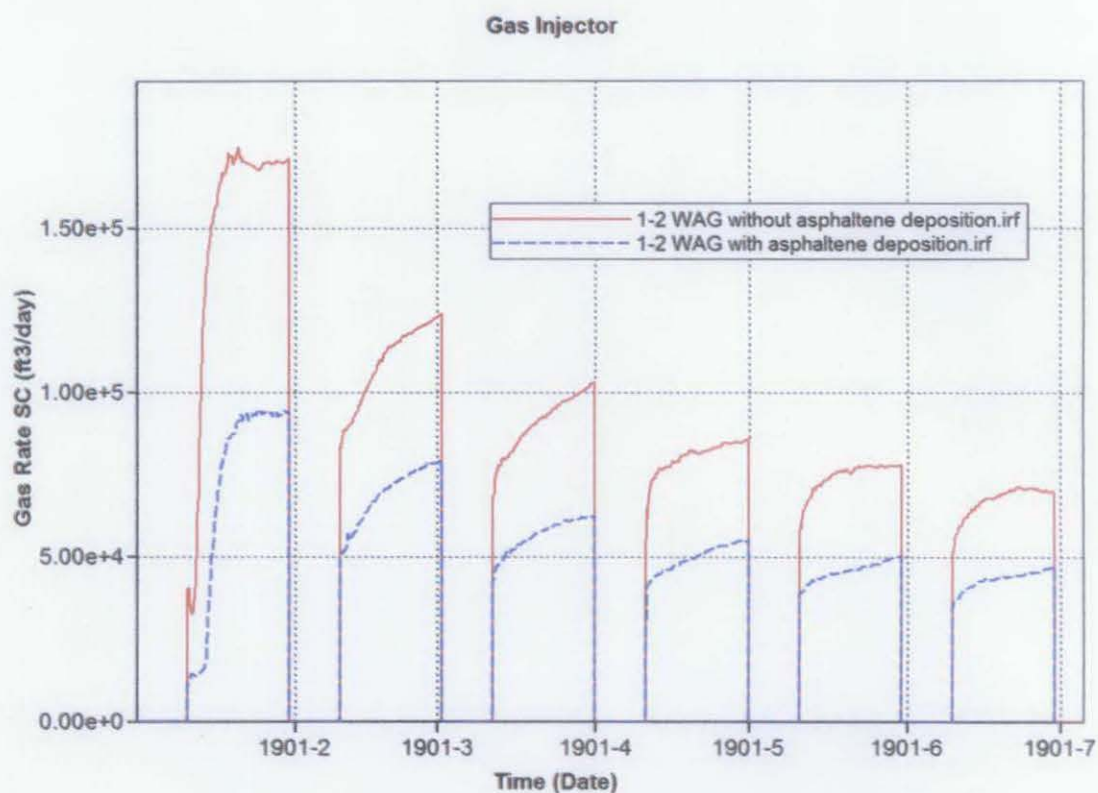


Figure 26: Injector gas rate, ft³/day vs. time

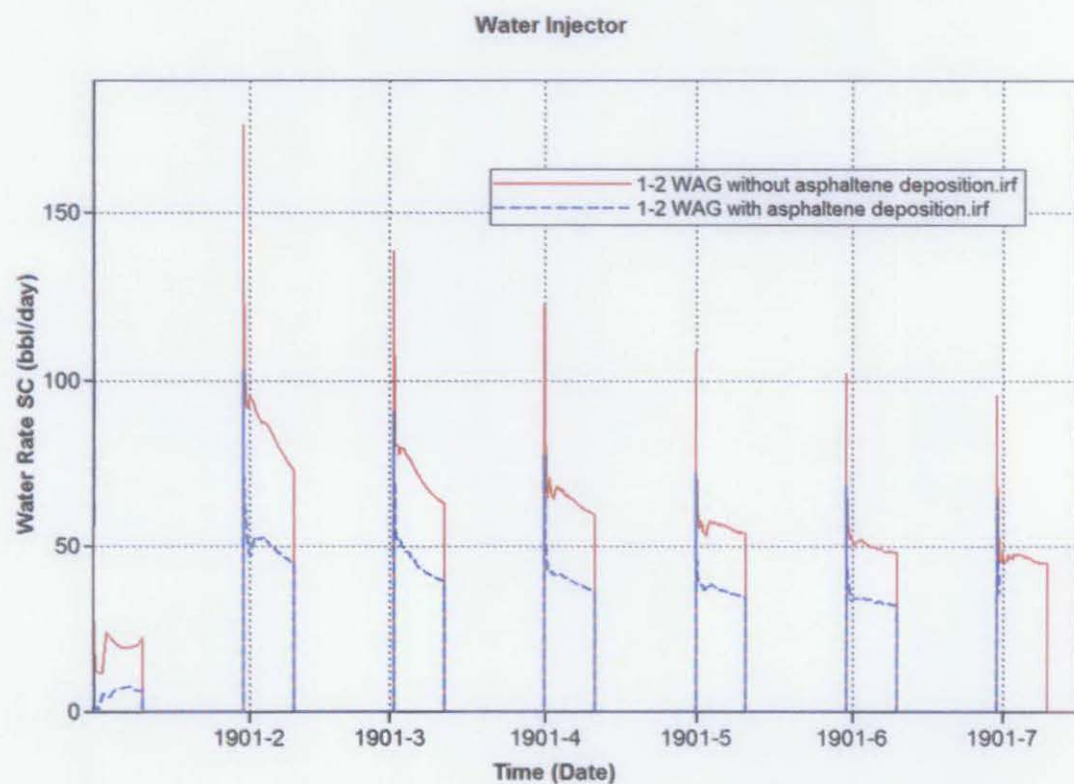


Figure 27: Injector water rate, bbl/day vs. time

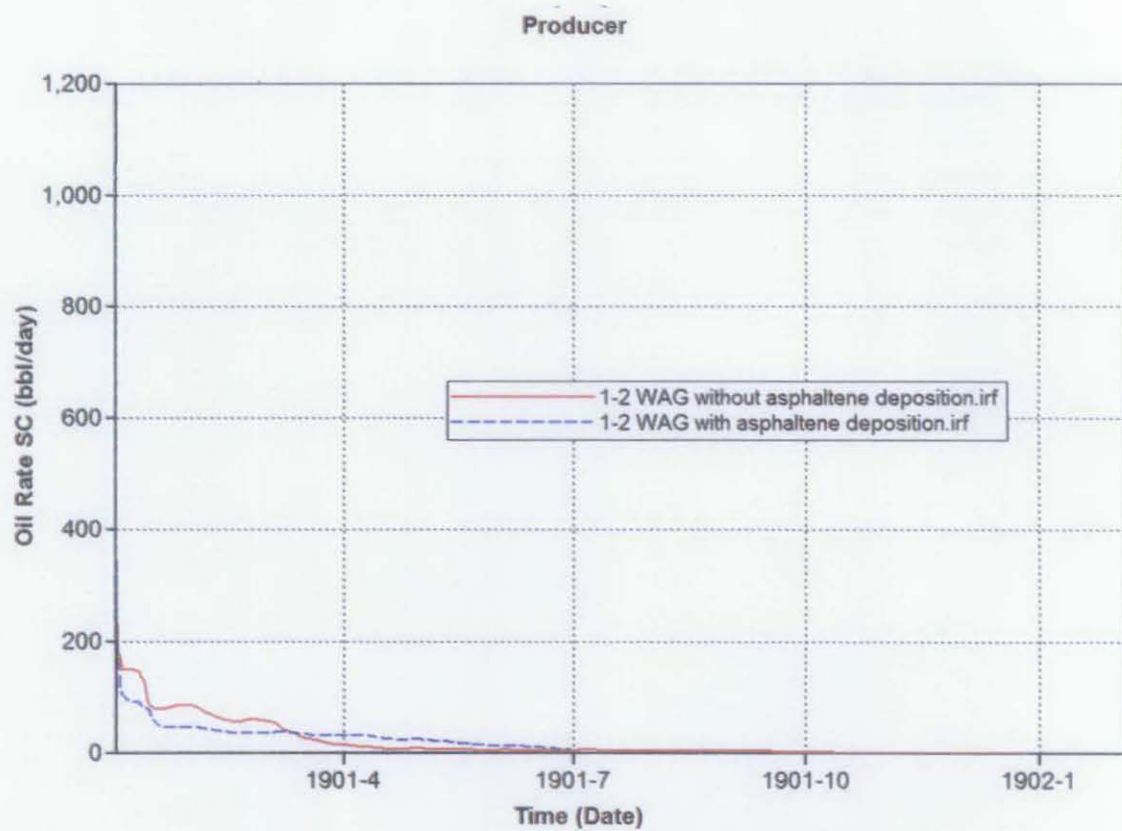


Figure 28: Producer oil rate, bbl/day vs. time

4.3.4 Viscous Fingering Simulation during 2:1 WAG Injection

In 2:1 WAG injection scheme, it started with 20 days of water injection followed by 10 days of CO₂ injection and then followed again by 20 days of water injection. The cycle keeps repeating until the simulation stops.

Below are the results:

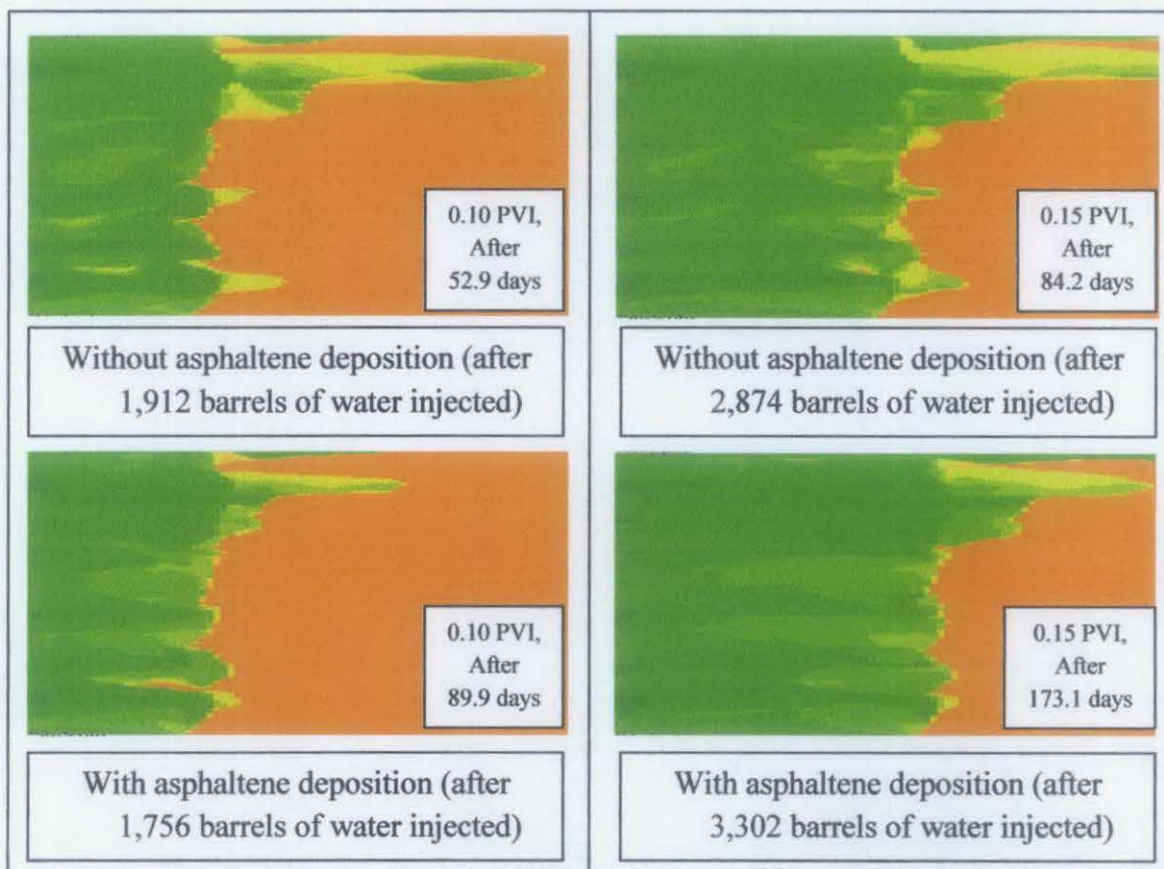


Figure 29: Oil saturation at 0.10 PVI (left) and 0.15 PVI (right)

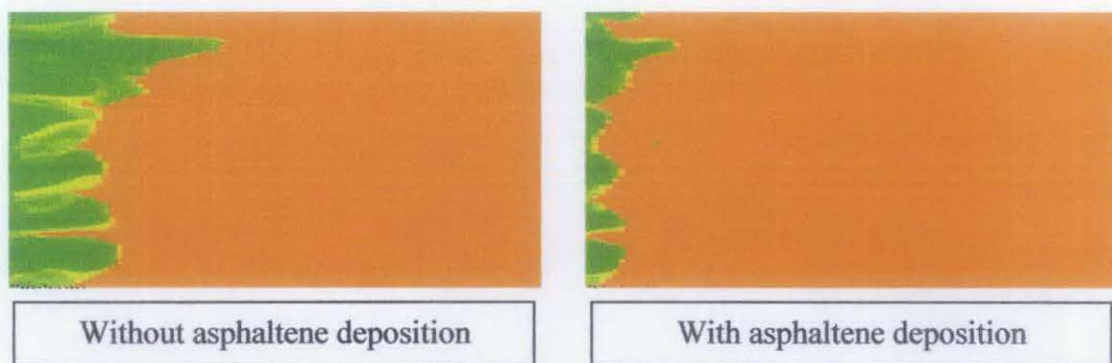


Figure 30: Oil saturation after 30 days of 2:1 WAG injection

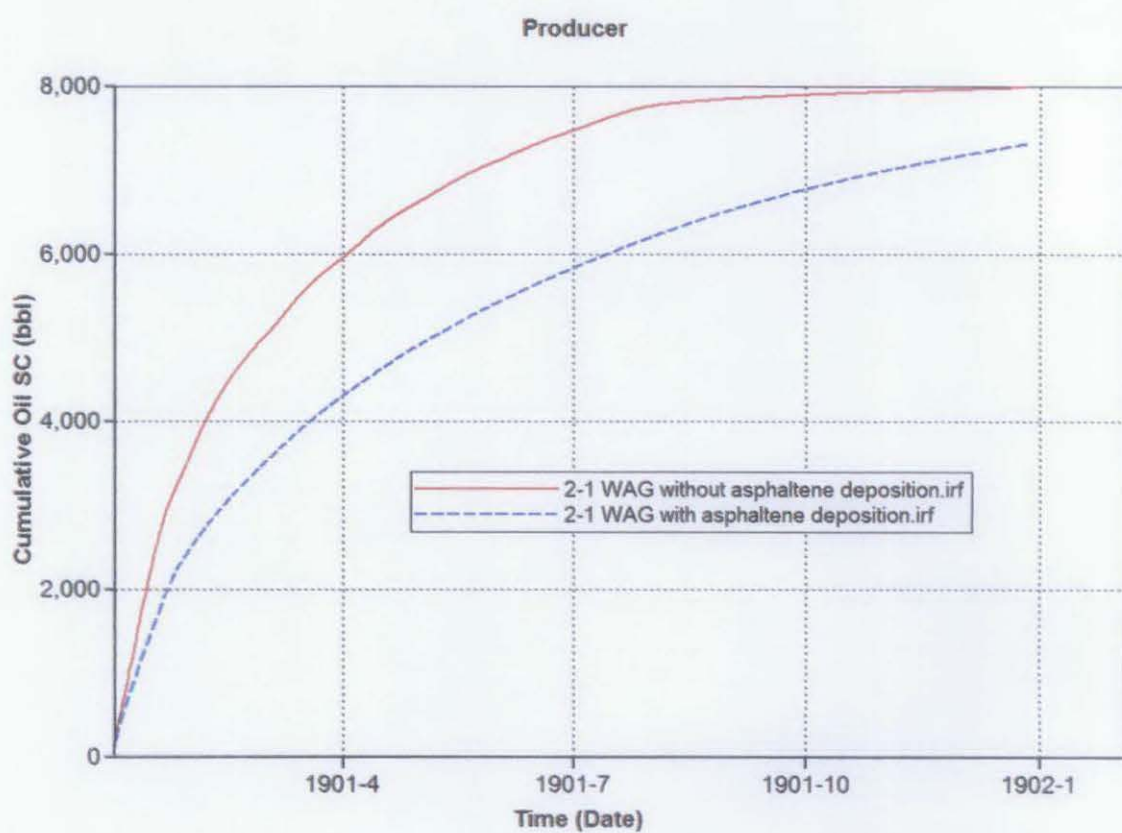


Figure 31: Cumulative oil produced, bbl vs. time

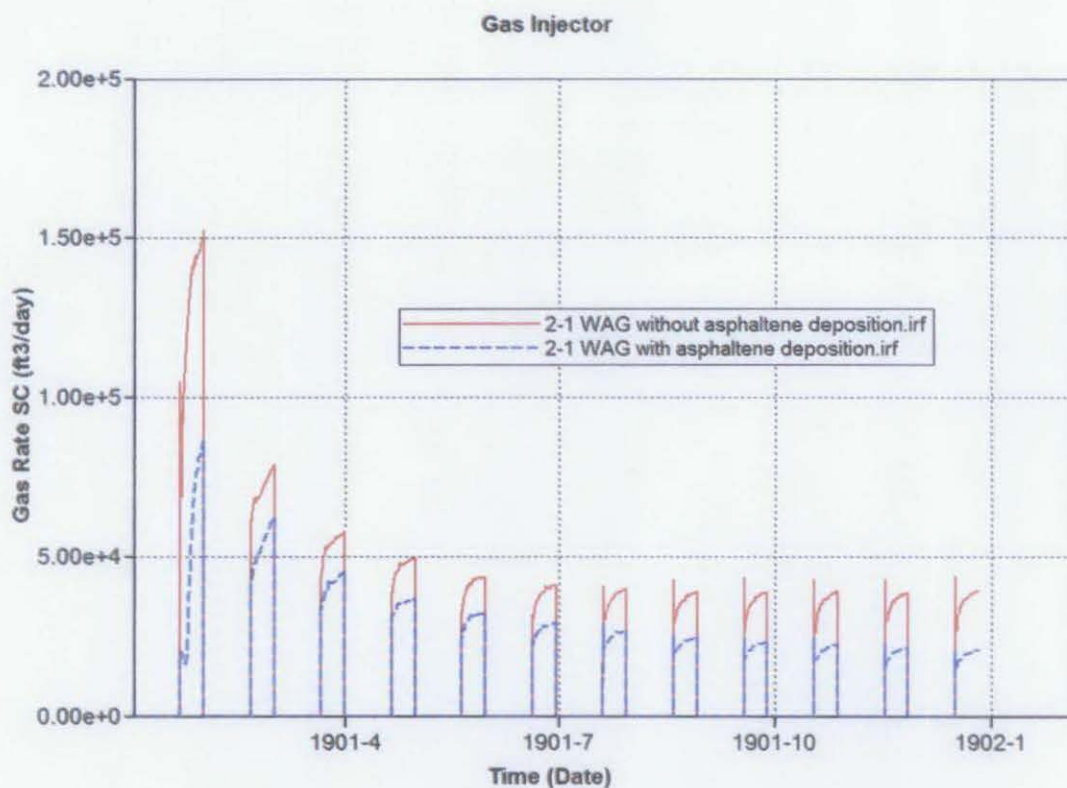


Figure 32: Injector gas rate, ft³/day vs. time

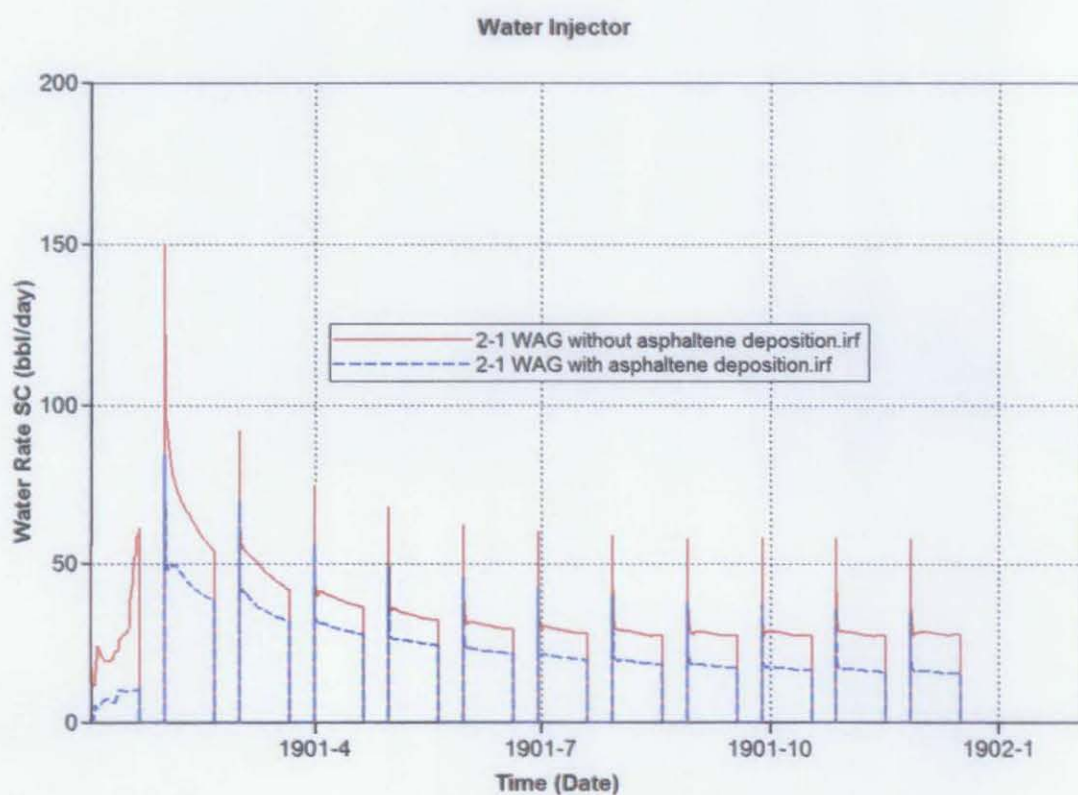


Figure 33: Injector water rate, bbl/day vs. time

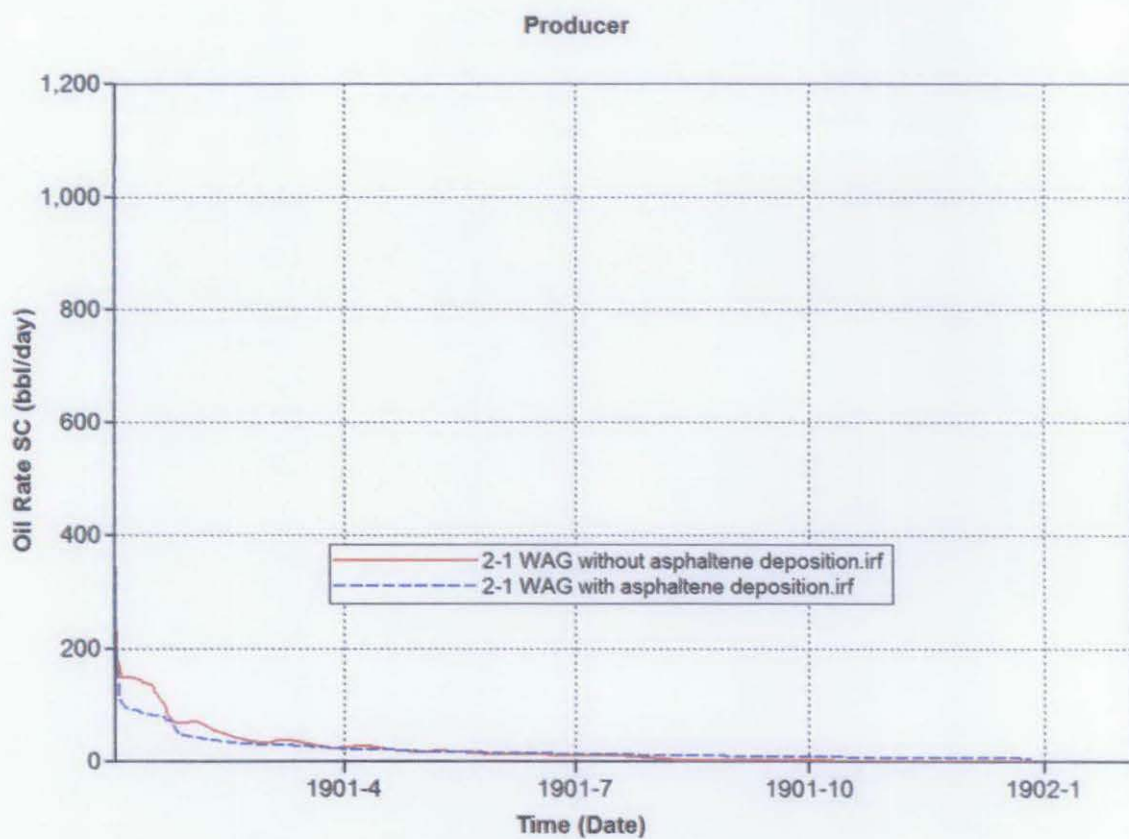


Figure 34: Producer oil rate, bbl/day vs. time

4.4 Discussion

In this section, simulation results of the 4 types of injection method are discussed. As stated earlier in this report, the objective of this study is to investigate the effect of asphaltene deposition on viscous fingering and oil recovery. The effect of asphaltene deposition on viscous fingering that has been studied was in terms of size, shape and speed of propagation. For each type of injection method, the viscous fingering in formation without asphaltene deposition is compared with the viscous fingering in formation with asphaltene deposition at the same PVI to see whether asphaltene deposition affects the shape and size of viscous fingering. The same comparison but at a similar amount of days injected is to see the effect of asphaltene deposition on propagation speed of viscous fingering. PVI refers to the pore volume injected by gas.

Based on Figure 13, Figure 18, Figure 24, and Figure 30, the propagation of viscous fingering is slower in the presence of asphaltene deposition for all the 4 types of injection method. This is the most noticeable effect of asphaltene deposition on viscous fingering and it can be explained by knowing how CMG GEM models the effect of permeability reduction due to asphaltene deposition. It is generally known that asphaltene deposition causes pore-throat plugging and permeability reduction. CMG GEM uses a simple model for these phenomena based on a resistance factor. The resistance factor relates the original permeability, k_0 to the instantaneous permeability, k as a function of the ratio of the original porosity to the instantaneous porosity. The permeability resistance factor used in CMG GEM is stated and explained in more detail earlier in Chapter 4.

Equation (8) mentioned earlier in this chapter is the equation for the resistance factor while Equation (9) is the equation for the instantaneous porosity. Based on Equation (9), increase in volume of deposited solid s_2 per gridblock volume will increase the value of resistance factor. The resistance factor is divided into each of the gas, oil and aqueous phase mobilities, thereby reducing the volumetric flow rates for all flowing phases in order to account for the reduced permeability due to asphaltene deposition. In

other words, the permeability reduction by adsorption of asphaltene on rock surface causes increase in permeability resistance factor for all the flowing phases which in turn decreasing their mobilities. These explain the slow propagation of viscous fingering in presence of asphaltene deposition. Figure 15, Figure 16, Figure 20, Figure 21, Figure 22, Figure 26, Figure 27, Figure 28, Figure 32, Figure 33 and Figure 34 shows the effect of asphaltene deposition on gas, water and oil rate.

Gas travels faster than water especially in high permeability zones. Therefore, in every WAG simulations conducted in this study, even though water is injected first, gas still travels ahead of water. The most noticeable propagation of gas is at the one section of upper part of the formation where horizontal permeability is the highest. Gas travels faster in that section while water travels quite uniformly in all section.

At a similar PVI, it is known that the amount of gas injected into the formation is also similar. Based on Figure 12, at 0.1 PVI and 0.2 PVI, no noticeable changes of fingering are observed in terms of shape and size between the formation with and without asphaltene deposition during CO₂ injection. Based on Figure 17, Figure 23, and Figure 29, for every types of WAG injection, the shape and size of viscous fingering is slightly different between the formation with and without presence of asphaltene deposition when compared at 0.10 PVI and 0.15 PVI.

Based on Figure 17, Figure 23, and Figure 29, viscous fingering is compared between the case of formation with and without asphaltene deposition for every WAG injection schemes at the same PVI. First thing to take note is at the same amount of PVI, for every type of WAG injection schemes, there are differences in the amount of water injected and the number of WAG cycle needed to achieve that PVI between the two cases.

As discussed earlier, asphaltene deposition causes permeability reduction which in turn reduces the volumetric flow rate of water, gas and oil in a formation. The reduced flow rate of injected water and gas caused by asphaltene deposition reduces the amount of water and gas injected into the formation in one WAG cycle which means, formation with asphaltene deposition needs more WAG cycles to achieve the same PVI as the formation without asphaltene deposition. For example, 0.20 PVI can be achieved after only 2 1:1 WAG cycles for the case of without asphaltene deposition but for the case of with asphaltene deposition, the number of 1:1 WAG cycle needed to achieve 0.20 PVI is 4. The higher number of WAG cycle needed by the formation with asphaltene deposition causes higher amount of water injected into the formation so less fingering is generally observed.

In addition, between CO₂ injection and WAG injection, viscous fingering is the worst in CO₂ injection since there is no injected water to suppress the fingering. Out of the 3 WAG schemes, viscous fingering is the worst in 1:2 WAG injection since the amount of gas injected in one cycle is the highest compared to other schemes. Fingering is successfully suppressed in 2:1 WAG injection because of the higher amount of injected water in one cycle.

The injected solvent and injected water naturally travel at different speeds. If much more solvent than water is injected, the solvent front moves ahead of the water and we see severe fingering of this solvent into the oil. If much more water than solvent is injected, the water moves ahead of the solvent. While this reduces the fingering, the recovery resembles that of a waterflood until the oil is contacted by the slow moving solvent front.

There is an optimum ratio of water to solvent injected called optimum WAG ratio, which minimizes the degree of fingering. Optimum WAG ratio is the value of injected fractional flow of water, f_{inj} at which the solvent and water fronts move at the same speed. However, this project does not include the simulation of WAG injection at the optimum WAG ratio since it does not directly relate to the objectives of this project.

This study does not investigate the effectiveness of different EOR methods but to show the effect of asphaltene deposition on oil recovery for each of the methods. Based on the cumulative oil produced vs. time plot below, asphaltene deposition slows down the rate of oil production for every EOR methods simulated. The dotted lines in the plot represent EOR in presence of asphaltene deposition. The same explanation goes for this case. Asphaltene deposition causes permeability reduction which increases the permeability resistance factor. Increase in permeability resistance factor causes the rate of all the flowing phases to reduce including oil.

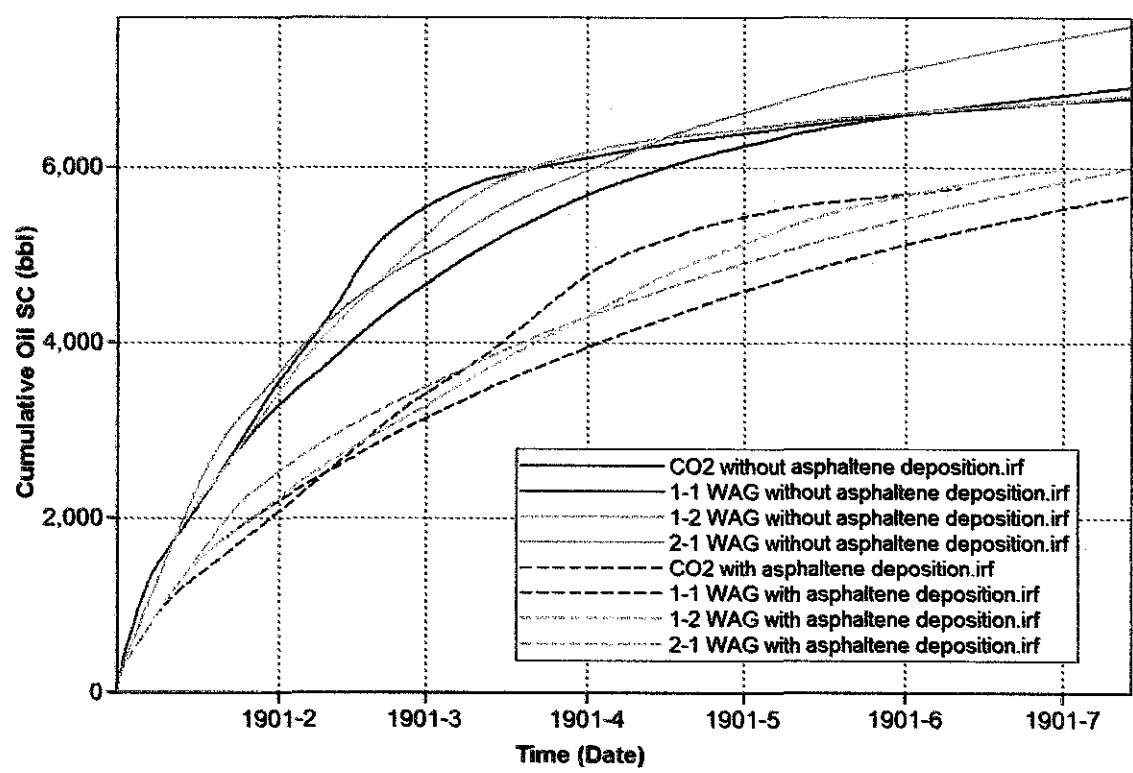


Figure 35: Cumulative oil produced, bbl vs. time for every types of EOR method

For the case of without presence of asphaltene deposition, the permeability resistance factor is 1 but for the case of with presence of asphaltene deposition, the factor is more than 1. Based on Equation (9) and Figure 36, permeability resistance factor is the function of the amount of deposited asphaltene. The resistance factor increases with the increase of deposited asphaltene volume.

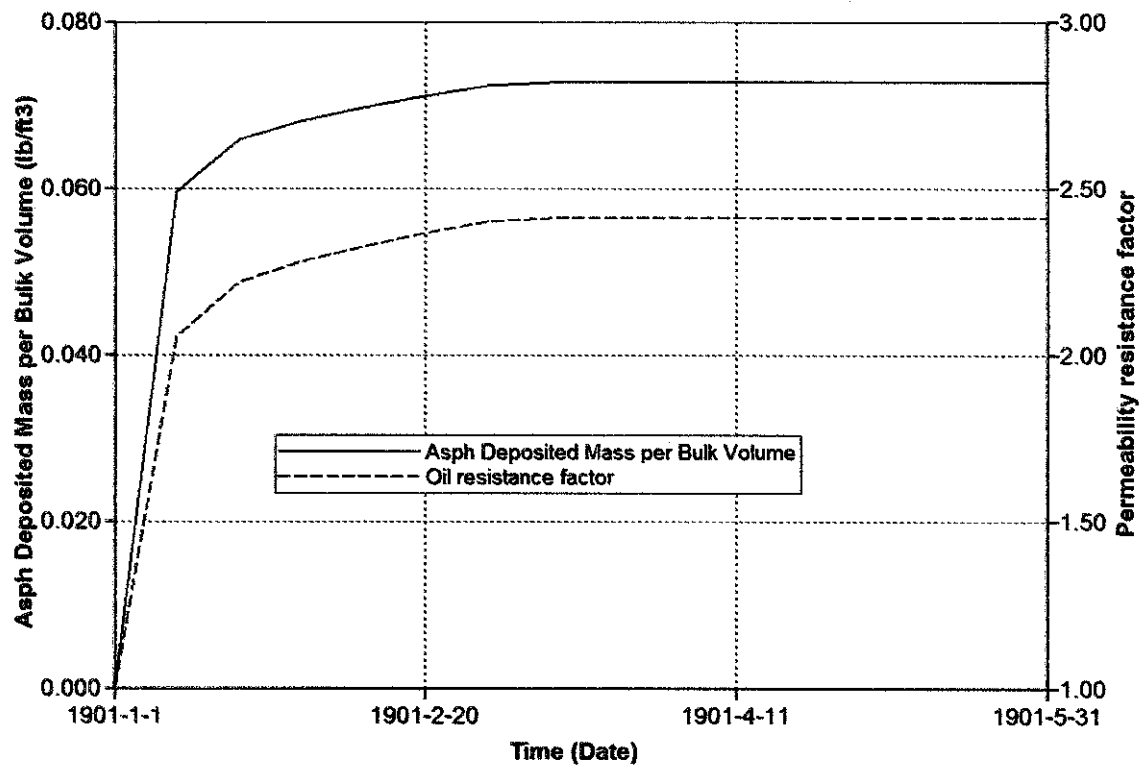


Figure 36: Development of solid deposition and permeability resistance factor for 1:1 WAG injection simulation

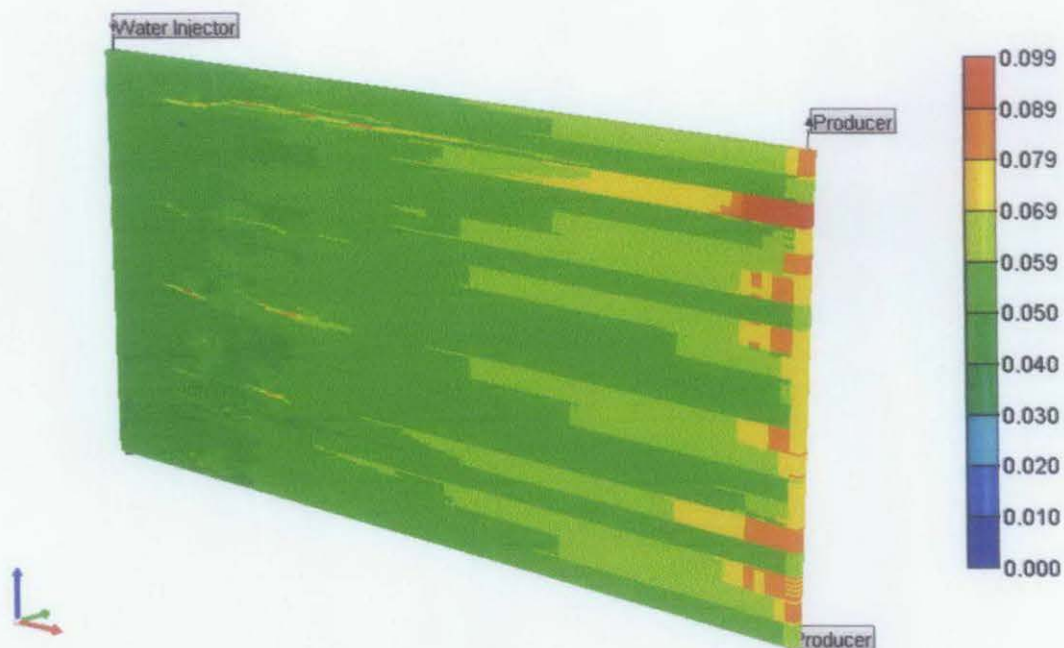


Figure 37: Distribution of asphaltene deposited mass per bulk volume (lb/ft³) after 80 days of 1:1 WAG injection

Figure 37 shows that general field observations which indicate the majority of asphaltene deposition problem occur in near-wellbore region are consistent with the CMG GEM simulation results.

4.5 Additional Simulations

In this section, results of additional simulations are presented and discussed. The purpose of conducting the additional simulations was to experiment with some of the simulation variables such as:

- i. Using homogeneous formation instead of heterogeneous formation
- ii. Using 1:3 and 3:1 WAG scheme
- iii. Removing grid refinement
- iv. Increasing the amount of deposited asphaltene in the formation

However, the results from these simulations were not incorporated with the results from the main simulations for discussion since the results from the main simulations are already enough to satisfy this project's objectives.

4.5.1 Viscous Fingering Simulation in Homogeneous Formation

Permeability distribution for homogeneous formation is attached at appendix section. This simulation was using Oil 1 as the fluid in the homogeneous formation.

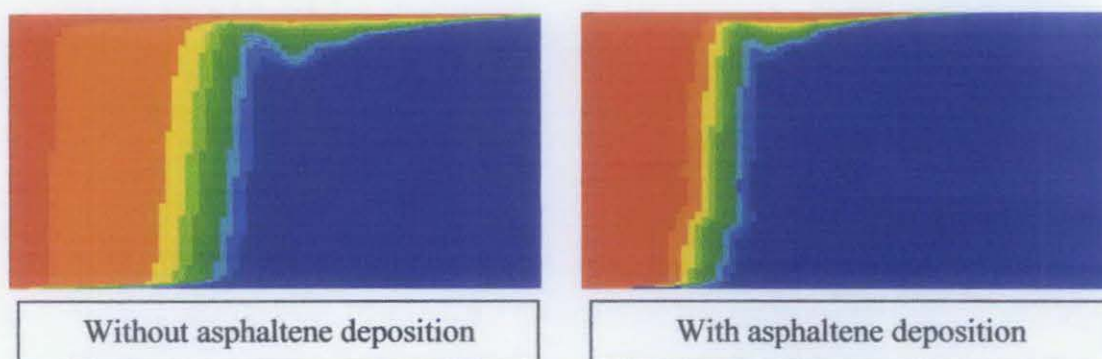


Figure 38: CO₂ distribution after 30 days of CO₂ injection in homogeneous formation

According to Figure 38, no viscous fingering is observed in homogeneous formation. Only gravity tongue is observed which is due to the gravity effect. Since gas is very low in density, injected gas migrates upward and sweep the upper part of the formation faster than the lower part which results in poor sweep efficiency. Permeability heterogeneity in a formation acts as a trigger for viscous fingering which in this case is absent.

4.5.2 Viscous Fingering Simulation during 1:3 WAG Injection

The simulation properties for 1:3 WAG injection is the same as the other WAG injection except for the injection cycle. 1:3 WAG injection consists of 10 days of water injection followed by 30 days of CO₂ injection which means more gas is injected than water in one cycle.

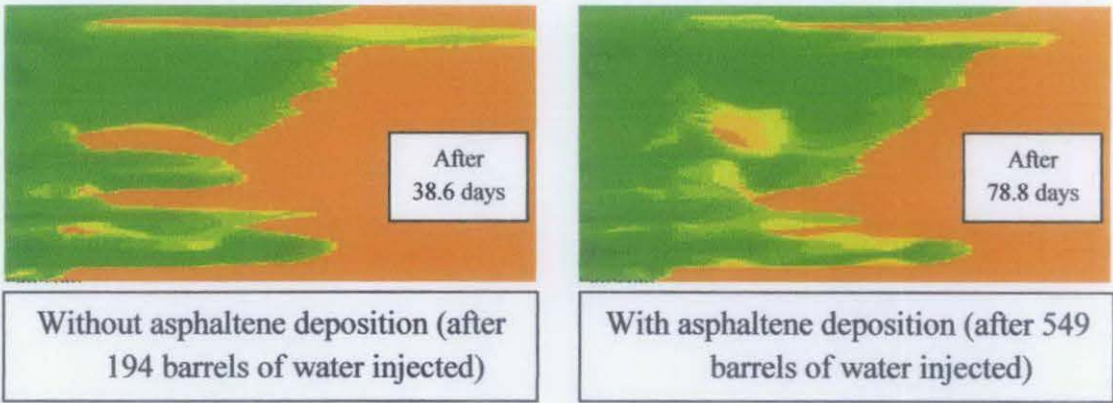


Figure 39: Oil saturation at 0.30 PVI

The viscous fingering in 1:3 WAG injection is the worst if compared to 1:1, 1:2, 2:1 and 3:1 WAG injection scheme because 1:3 WAG injection has the highest amount of CO₂ injection in one WAG cycle. Higher amount of water injection are needed to reduce the degree of viscous fingering or in other words higher WAG ratio is needed.

4.5.3 Viscous Fingering Simulation during 3:1 WAG Injection

The simulation properties for 3:1 WAG injection is also the same as the other WAG injection except for the injection cycle. 3:1 WAG injection consists of 30 days of water injection followed by 10 days of CO₂ injection which means more water is injected than gas in one cycle.

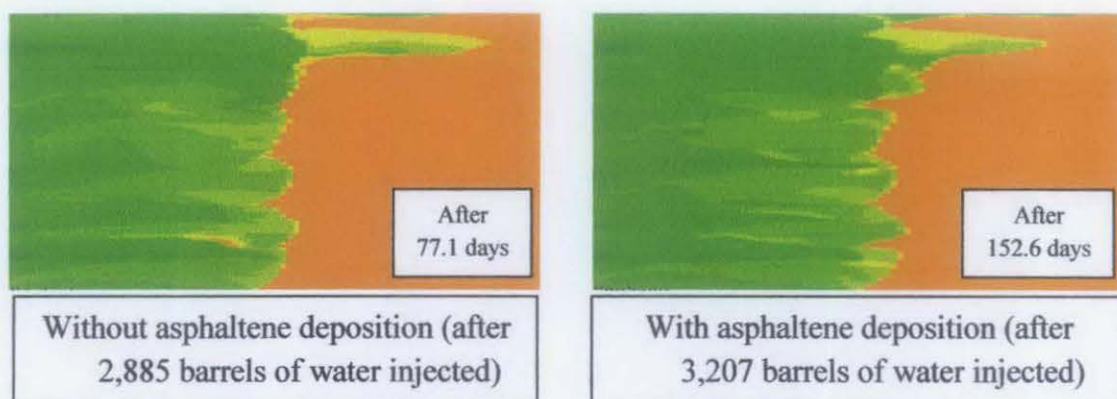


Figure 40: Oil saturation at 0.10 PVI

The results show that amount of viscous fingering is decreased with increasing WAG ratio meaning higher amount of water injected compared to gas in one cycle. Water injection helps to reduce the amount of viscous fingering in the reservoir by decreasing the apparent mobility contrast between the injected and displaced fluids hence improving sweep efficiency. ^[5]

4.5.4 Viscous Fingering Simulation without Grid Refinement

The default amount of grid block for the main simulations for this project is 17,600. In this simulation, the effect of number of grid block for exactly the same formation is studied. To achieve the objective, grid refinement was removed which resulted in the number of grid block to only 1,600.

The type of injection method for this simulation is 2:1 WAG injection scheme in a formation without asphaltene deposition. Below are the results:

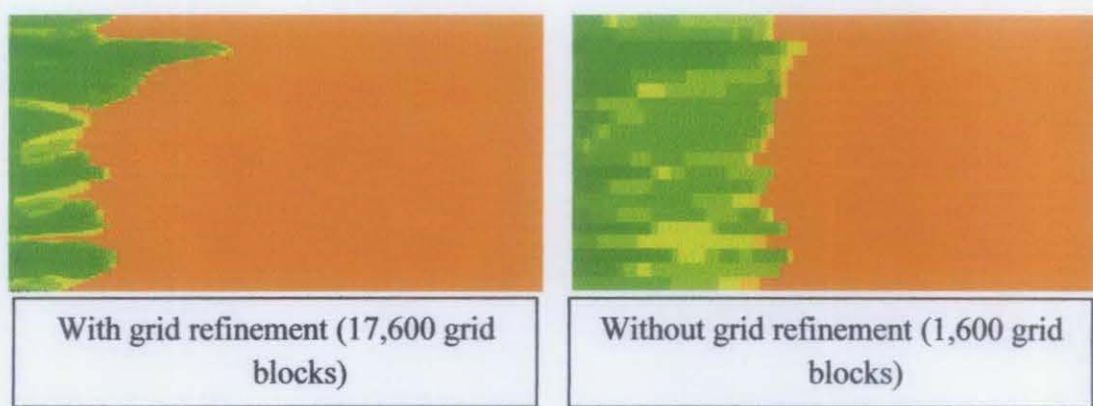


Figure 41: Oil saturation at after 30 days of 2:1 WAG injection

From the above figure, the most noticeable difference between the two simulations is the detail of viscous fingering which is more refined in the case of with grid refinement due to higher amount of grid block used. The second noticeable difference is the propagation of viscous fingering in the case of without grid refinement is faster than the one in the case of with grid refinement. After 30 days of WAG injection, the amount of PVI in the case without grid refinement is larger.

Due to the critical differences between the two simulations, in order to accurately compare the viscous fingering in this project, the number of grid block used must be kept constant. Number of grid block must be high enough to simulate viscous fingering in detail.

4.5.5 Higher Amount of Asphaltene Deposition

In CMG GEM, the amount of asphaltene deposition can be controlled using a certain keywords in the data file. 'SOLID-CONV-RATE' keyword specifies the amount of forward reaction rate (1/day) for the conversion of precipitated asphaltene to flocculated asphaltene particles and backward reaction rate (1/day) for the conversion of flocculated asphaltene particles back to precipitated asphaltene. 'SOLID_ALPHA' keyword specifies the surface deposition rate constant (1/day).

In this case, the value for 'SOLID-CONV-RATE' and 'SOLID_ALPHA' was increased from 2 to 1000. Below are the results:

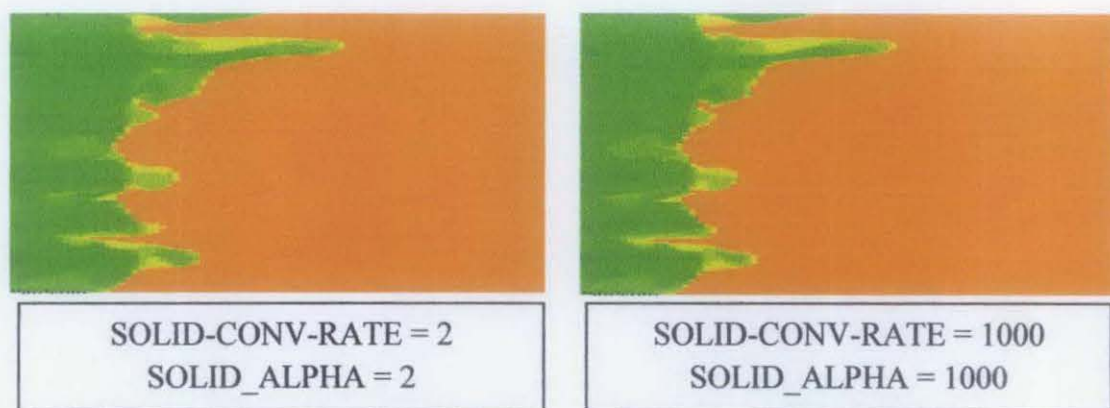


Figure 42: Oil saturation after 60 days of 1:1 WAG injection

Based on the above figure, no significant changes in size and shape of viscous fingering can be observed. However, if closely observed, the viscous fingering in the case with higher value of 'SOLID-CONV-RATE' and 'SOLID_ALPHA' propagates just a little bit slower compared to the other case. This is due to the slightly higher amount of asphaltene deposition volume increases the permeability resistance factor a bit which slows down the propagation of viscous fingering a little more. The changes are almost unnoticed maybe because by using the value of only 2, the maximum amount of asphaltene precipitation and deposition can already been achieved since the amount of asphaltene content in the oil used is relatively minute which is 1.7 wt%. Any increase in the value above 2 makes no appreciable effect on viscous fingering.

CHAPTER 5

CONCLUSION AND RECOMMENDATION

5.1 Conclusion

The most important and noticeable effect of asphaltene deposition on viscous fingering is the slow propagation of viscous fingering which is due to the increase in permeability resistance factor. Asphaltene deposition slows down the volumetric flow rate of all the flowing phases in a formation which explains the slow propagation of injected water and gas and also the slow production of oil.

At a similar PVI, presence of asphaltene deposition does not affect the size and shape of viscous fingering in CO₂ injection. In WAG injection, at a similar PVI, presence of asphaltene deposition changes slightly the shape and size of viscous fingering due to permeability resistance factor and the degree of changes varies upon the type of WAG injection scheme.

No viscous fingering is observed in homogeneous formation. Only gravity tongue can be observed where lighter gas migrates upward in the formation which is the result of density difference between gas and oil. Formation must be heterogeneous where permeability distribution is varied across the formation in order to initiate the viscous fingering. Less fingering is observed at high WAG ratio and vice versa.

CMG has provided an easy to use set of simulation software. With various advanced features offered and very good software support, the use of CMG as an alternative to ECLIPSE by Schlumberger is recommended.

5.2 Recommendations

Since asphaltene deposition causes pore-throat plugging and permeability reduction which in turn slows down the flowing phases in a formation, it must be avoided.

This study was conducted using 2D simulation. For future work, 3D simulation could be done instead of 2D simulation to see if there are any differences in results between them. Experimental study is highly recommended to see the effect of viscous fingering during WAG in presence of asphaltene deposition. The results from the experimental study can be compared with the results from this study and might support each other.

REFERENCES

- [1] John R. Fanchi, 2006. *Principles of Applied Reservoir Simulation*. 3rd ed. Elsevier.
- [2] Abdallah, D., Al-Basry, A., Zwolle, S., Grutters, M., Huo, Z., & Stankiewicz, A., "Asphaltene Studies in On-shore Abu Dhabi Oil Fields, PART II: Investigation and Mitigation of Asphaltene Deposition – A Case Study" Abu Dhabi International Petroleum Exhibition & Conference, Abu Dhabi, UAE, 1 – 4 November 2010.
- [3] G. P. Oskui, M.A. Jumaa, W. A. Abuhaimeed, "Laboratory Investigation of Asphaltene Precipitation Problems during CO₂/Hydrocarbon Injection Project for EOR Application in Kuwait Reservoirs" Kuwait International Conference and Exhibition-Kuwait City, 14 – 16 December 2009.
- [4] enhanced oil recovery, viewed on April 1st 2011, <http://www.glossary.oilfield.slb.com/Display.cfm?Term=enhanced%20oil%20recovery>
- [5] Blunt, M., & Christie, M., "How to Predict Viscous Fingering in Three Component Flow" *Transport in Porous Media* 12: 207 – 236, Kluwer Academic Publishers, 1993.
- [6] De Boer, R.B., Leerlooyer, K., Eigner, M.R.P., & van Bergen, A.R.D., "Screening of Crude Oils for Asphalt Precipitation: Theory, Practice, and the Selection of Inhibitors" SPE Paper 24987 first presented at SPE European Petroleum Conference, Cannes, Nov. 16 – 18, 1992.
- [7] Stalkup, F.I., 1983. *Miscible Flooding*, SPE Monograph 8, Richardson, TX.
- [8] Naami, A.M., Catania, P., & Islam, M.R., "Numerical and Experimental Modeling of Viscous Fingering in Two-Dimensional Consolidated Porous Medium" 8th Petroleum Conference of the South Saskatchewan Section, Petroleum Society of CIM, 18 – 21 October, 1999.
- [9] Juanes, R., & Blunt, M.J., "Impact of Viscous Fingering on the Prediction of Optimum WAG Ratio" SPE Paper 99721 presented at 2006 SPE/DOE Symposium on Improved Oil Recovery, Tulsa, 22 – 26 April, 2006.

- [10] Tchelepi, H.A., & Orr. Jr., F.M., "Interaction of Viscous Fingering, Permeability Heterogeneity, and Gravity Segregation in Three Dimensions" SPE Paper 25235 presented at the 1993 SPE Symposium on Reservoir Simulation, New Orleans, Feb. 28 – March 3, 1993.
- [11] Moissis, D.E., Miller, C.A., and Wheeler, M.F., 1988. "A Parametric Study of Viscous Fingering in Miscible Displacement by Numerical Simulation" *Numerical Simulation in Oil Recovery*, 227 – 247.
- [12] Ku, Hwar-Ching, Hirsh, R.S., & Taylor, T.D., "Simulation of Viscous Fingering by the Pseudospectral Matrix" prepared for presentation at the SPE Symposium on Reservoir Simulation in Houston, TX, February 6 – 8, 1989.
- [13] Todd, M.R., Claridge, E.L., Almeida, J., Alvarez, R., & Echeverria, I., "Mechanistic Study of Alternative Gas Injection Processes for Enhanced Oil Recovery in the Los Jabillos (Cretaceous) Reservoir, Furrial Field, Norte Monagas, Venezuela" prepared for presentation at the 1999 SPE Latin American and Caribbean Petroleum Engineering Conference, Caracas, Venezuela, 21 – 23 April, 1999.
- [14] Takahashi, S., Hayashi, Y., Takahashi, S., Yazawa, N., Sarma, H., "Characteristics and Impact of Asphaltene Precipitation during CO₂ Injection in Sandstone and Carbonate Cores: An Investigative Analysis through Laboratory Tests and Compositional Simulation" prepared for presentation at the SPE International Improved Oil Recovery Conference in Asia Pacific, Kuala Lumpur, Malaysia, 20 – 21 October, 2003.
- [15] Henri Cholet, 2008. *Well Production Practical Handbook*. 2nd ed. Technip Editions. page 413.
- [16] Sarma, H.K., "Can We Ignore Asphaltene in a Gas Injection Project for Light-Oils?" prepared for presentation at SPE International Improved Oil Recovery Conference in Asia Pacific, Kuala Lumpur, Malaysia, 20 – 21 October, 2003.
- [17] Alta'ee, A.F., Saaïd, I.M., & Masoudi, R., "Carbon Dioxide Injection and Asphaltene Precipitation in Light Oil Reservoirs" The Eleventh Mediterranean Petroleum Conference and Exhibition, Tripoli – Libya, February 23 – 25, 2010.

- [18] J. Moghadasi, A.M. Kalantari-Dahaghi, V. Gholami, R. Adi, 2006 "Formation Damage Due to Asphaltene Precipitation Resulting from CO₂ Gas Injection in Iranian Carbonate Reservoirs" SPE Europec/EAGE Annual Conference and Exhibition, Vienna, Austria, 12 – 15 June, 2006.
- [19] Leontaritis, K.J., Amaefule, J.O., & Charles, R.E., "A Systematic Approach for the Prevention and Treatment of Formation Damage Caused by Asphaltene Deposition" SPE Paper 23810 presented at SPE Formation Damage Control Symposium, 1992.
- [20] Forrest F. Craig Jr., 1993. *The Reservoir Engineering Aspects of Waterflooding*. 3rd vol. Monograph Series, SPE, Richardson, TX.
- [21] *Enhanced Oil Recovery Scoping Study*, EPRI, Palo Alto, CA: 1999. TR-113836.
- [22] Burke, Hobbs and Kashou, "Measurement and Modeling of Asphaltene Precipitation" SPE Paper 18273 first presented at SPE Annual Technical Conference and Exhibition, Houston, October 2 – 5, 1988. *Journal of Petroleum Technology*, November 1990, pp. 1440-1446.
- [23] Blunt, M.J., Barker, J.W., Rubin, B., Mansfield, M., Culverwell, I.D., Christie, M.A., "Predictive Theory for Viscous Fingering in Compositional Displacement" SPE Paper 24129 first presented at the SPE Symposium on Enhanced Oil Recovery, Tulsa, April 22 – 24, 1992.
- [24] Todd, M.R. and Longstaff, W.J.: "The Development, Testing, and Application of a Numerical Simulator for Predicting Miscible Flood Performance," SPE Paper 3484 presented at SPE 46th Annual Fall Meeting, New Orleans, October 3 – 6, 1971.
- [25] Moissis, D.E., Wheeler, M.F., & Miller C.A., "Simulation of Miscible Viscous Fingering using a Modified Method of Characteristics: Effects of Gravity and Heterogeneity" SPE Advanced Technology Series, Vol. 1, No. 1, pp. 62-70.
- [26] Srivastava, R.K., Huang, S.S., Dong, M., "Asphaltene Deposition during CO₂ Flooding" SPE Prod. & Facilities, Vol. 14, November 1999, pp. 235-245.
- [27] Christie, M.A., Muggeridge, A.H., & Barley, J.J., "3D Simulation of Viscous Fingering and WAG Schemes" SPE Reservoir Engineering 1993, pp. 19-26.

- [28] Wang, S., & Civan, F., "Productivity Decline of Vertical and Horizontal Wells by Asphaltene Deposition in Petroleum Reservoirs," Paper SPE 64991, Proceedings 2001 SPE International Symposium on Oilfield Chemistry, Houston, TX, 13 – 16 February, 2001.
- [29] Reis, J.C., & Acock, A.M., "Permeability Reduction Models for the Precipitation of Inorganic Solids in Berea Sandstone," *In Situ* (1994) 18, No. 3, 347 – 368.
- [30] Jai Ying, Sun Lei, Sun Liangtian, Huang Lei, Huang Chunxia, & Hong Lin, "The Research on Asphaltene Deposition Mechanism and Its Influence on Development During CO₂ Injection", SPE paper 104417 presented at the 2006 SPE International Oil & Gas Conference and Exhibition, China, 5 – 7 December 2006.
- [31] Kohse, B.F., & Nghiem, L.X., "Modelling of Asphaltene Precipitation and Deposition in a Compositional Oil Simulator", Paper SPE 89437, prepared for presentation at the 2004 SPE/DOE Fourteenth Symposium on Improved Oil Recovery, Tulsa, Oklahoma, U.S.A., 17 – 21 April, 2004.

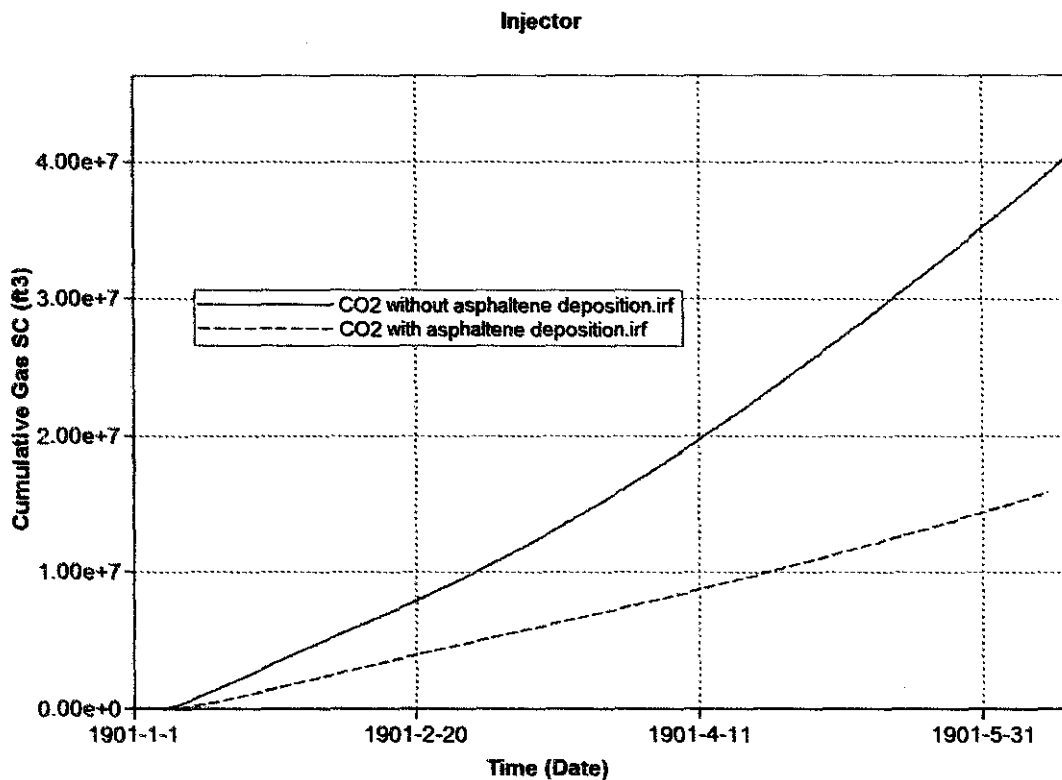
APPENDICES

| | Permeability I | Permeability J | Permeability K |
|-------------|----------------|----------------|----------------|
| UNITS: | md | md | md |
| SPECIFIED: | X | X | X |
| HAS VALUES: | X | X | X |
| Whole Grid | | | |
| Layer 1 | 150 | 150 | 100 |
| Layer 2 | 150 | 150 | 100 |
| Layer 3 | 150 | 150 | 100 |
| Layer 4 | 150 | 150 | 100 |
| Layer 5 | 150 | 150 | 100 |
| Layer 6 | 150 | 150 | 100 |
| Layer 7 | 150 | 150 | 100 |
| Layer 8 | 150 | 150 | 100 |
| Layer 9 | 150 | 150 | 100 |
| Layer 10 | 150 | 150 | 100 |
| Layer 11 | 150 | 150 | 100 |
| Layer 12 | 150 | 150 | 100 |
| Layer 13 | 150 | 150 | 100 |
| Layer 14 | 150 | 150 | 100 |
| Layer 15 | 150 | 150 | 100 |
| Layer 16 | 150 | 150 | 100 |
| Layer 17 | 150 | 150 | 100 |
| Layer 18 | 150 | 150 | 100 |
| Layer 19 | 150 | 150 | 100 |
| Layer 20 | 150 | 150 | 100 |

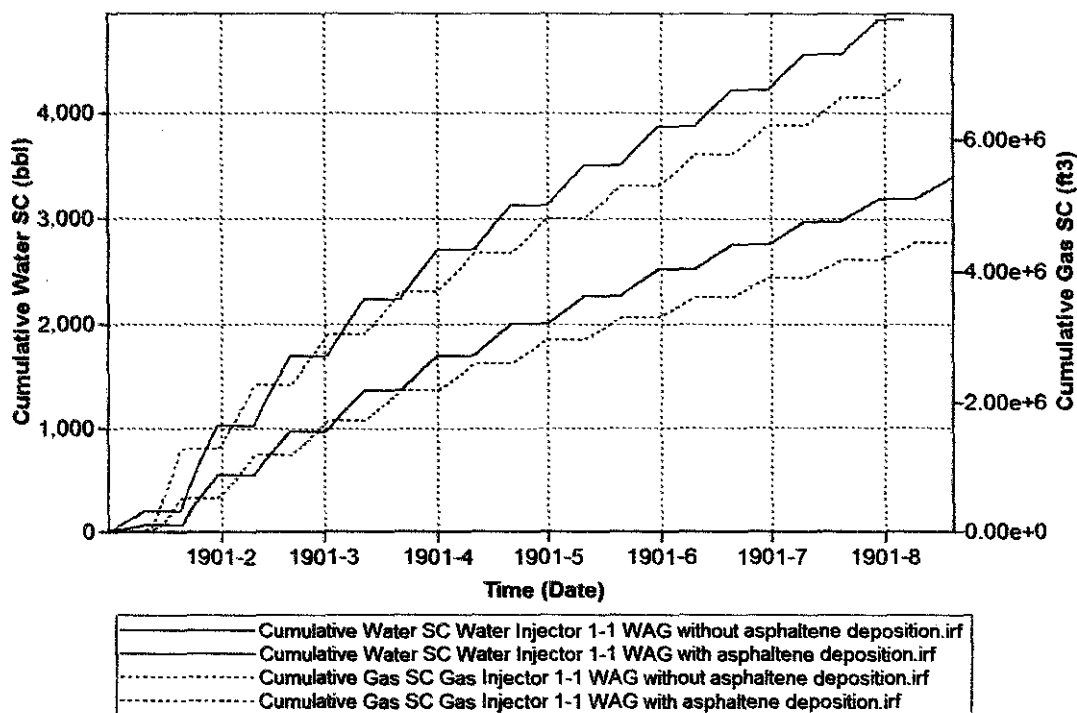
1. PERMEABILITY DISTRIBUTION FOR HOMOGENEOUS FORMATION

| | Permeability I | Permeability J | Permeability K |
|-------------|----------------|----------------|----------------|
| UNITS: | md | md | md |
| SPECIFIED: | X | X | X |
| HAS VALUES: | X | X | X |
| Whole Grid | | | |
| Layer 1 | 100 | 60 | 45 |
| Layer 2 | 30 | 11 | 11 |
| Layer 3 | 300 | 223 | 9 |
| Layer 4 | 45 | 156 | 69 |
| Layer 5 | 100 | 111 | 11 |
| Layer 6 | 150 | 54 | 15 |
| Layer 7 | 16 | 67 | 15 |
| Layer 8 | 150 | 33 | 17 |
| Layer 9 | 67 | 100 | 24 |
| Layer 10 | 39 | 189 | 17 |
| Layer 11 | 34 | 240 | 5 |
| Layer 12 | 150 | 110 | 25 |
| Layer 13 | 95 | 10 | 15 |
| Layer 14 | 24 | 155 | 20 |
| Layer 15 | 55 | 91 | 5 |
| Layer 16 | 201 | 56 | 15 |
| Layer 17 | 10 | 19 | 5 |
| Layer 18 | 167 | 120 | 5 |
| Layer 19 | 100 | 67 | 20 |
| Layer 20 | 24 | 11 | 16 |

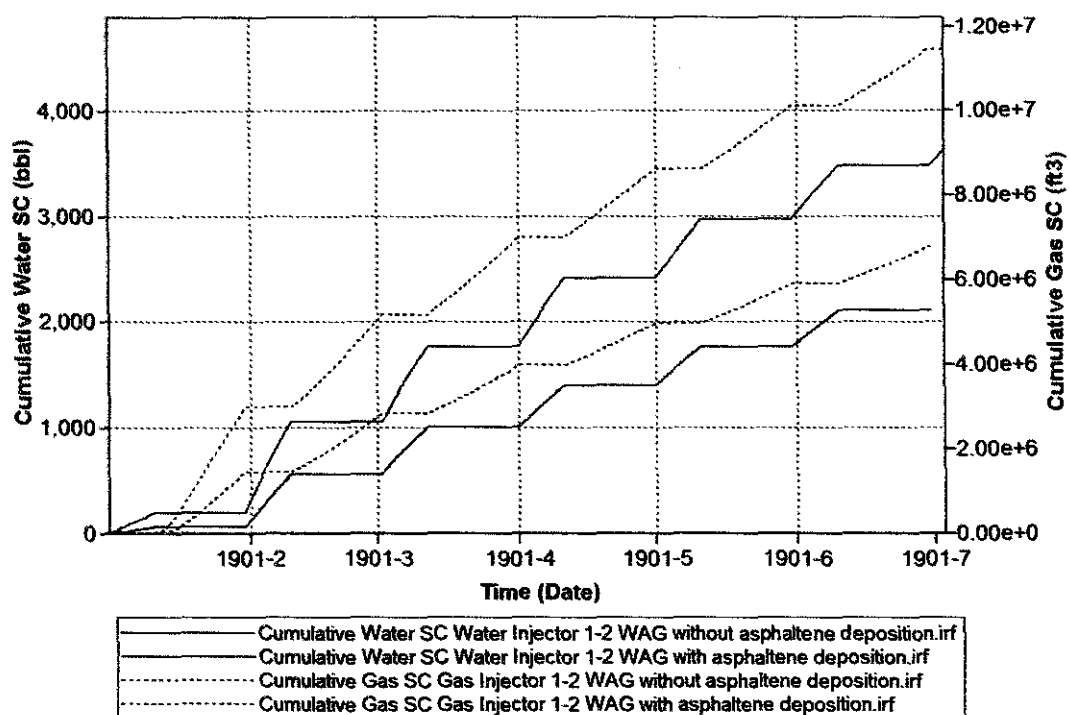
2. PERMEABILITY DISTRIBUTION FOR HETEROGENEOUS FORMATION



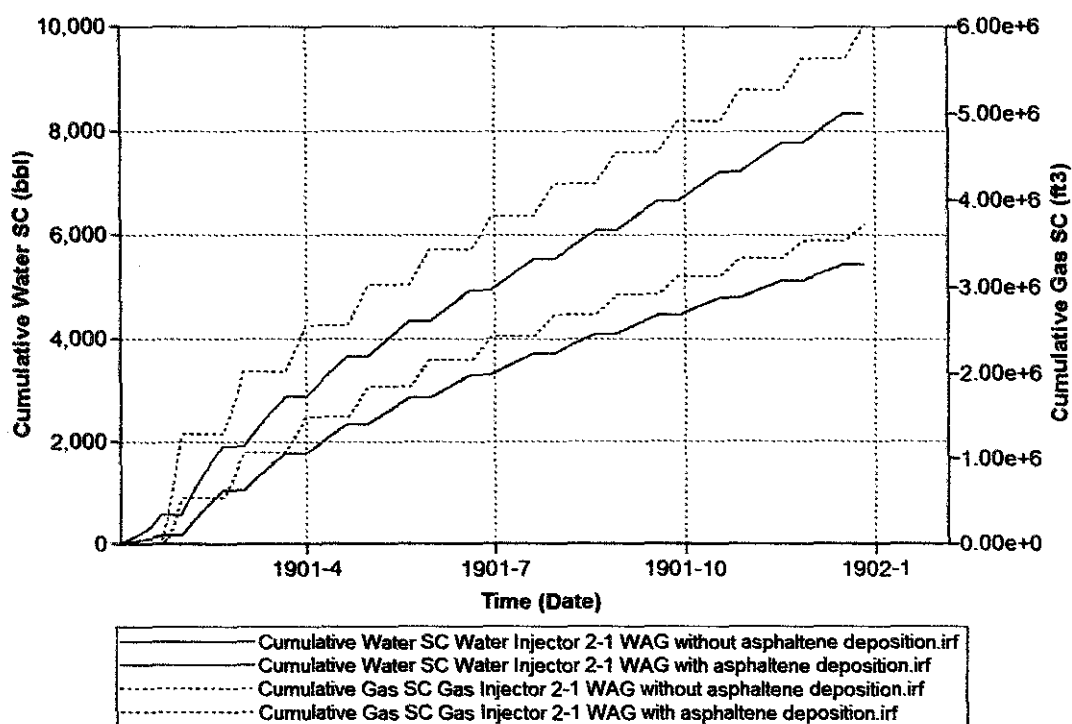
3. CUMULATIVE GAS INJECTED VS. TIME FOR CO2 INJECTION



4. CUMULATIVE WATER AND GAS INJECTED VS. TIME FOR 1:1 WAG INJECTION



5. CUMULATIVE WATER AND GAS INJECTED VS. TIME FOR 1:2 WAG INJECTION



6. CUMULATIVE WATER AND GAS INJECTED VS. TIME FOR 2:1 WAG INJECTION